

# 000 001 002 003 004 005 006 007 008 009 010 011 012 013 014 015 016 017 018 019 020 021 022 023 024 025 026 027 028 029 030 031 032 033 034 035 036 037 038 039 040 041 042 043 044 045 046 047 048 049 050 051 052 053 TOWARD CONSERVATIVE PLANNING FROM PREFERENCES IN OFFLINE REINFORCEMENT LEARNING

Anonymous authors

Paper under double-blind review

## ABSTRACT

We study offline reinforcement learning (RL) with trajectory preferences, where the RL agent does not receive explicit rewards at each step but instead receives human-provided preferences over pairs of trajectories. Despite growing interest in preference-based reinforcement learning (PbRL), contemporary works cannot robustly learn policies in offline settings with poor data coverage and often lack algorithmic tractability. We propose a novel **Model-based Conservative Planning** (MCP) algorithm for offline PbRL, which leverages a general function class and uses a tractable conservative learning framework to improve the policy upon an arbitrary reference policy. We prove that, MCP can compete with the best policy within data coverage when the reference policy is supported by the data. To the best of our knowledge, MCP is the first provably sample-efficient and computationally tractable offline PbRL algorithm under partial data coverage, without requiring known transition dynamics. We further demonstrate that, with certain structural properties in PbRL dynamics, our algorithm can effectively exploit these structures to relax the partial data coverage requirement and improve regret guarantees. We evaluate MCP on a comprehensive suite of human-in-the-loop benchmarks in Meta-World. Experimental results show that our algorithm achieves competitive performance compared to state-of-the-art offline PbRL algorithms.

## 1 INTRODUCTION

Reinforcement learning (RL) has become a prominent framework for addressing sequential decision-making problems. Most of the existing RL algorithms typically assume access to a well-defined reward function that guides policy optimization. However, in many practical applications, the design of an appropriate reward function poses a significant challenge. This difficulty arises from the complexity of accurately capturing human intent, the susceptibility to reward hacking, and the risk of inducing unintended behaviors due to mis-specified objectives [Wirth et al., 2017]. To tackle the problems, the framework of the preference-based reinforcement learning (PbRL) has emerged as a possible solution. Rather than relying on numerical reward signals, PbRL leverages relative preferences obtained from human experts or large language models, thereby avoiding explicitly modeling the reward function [Christiano et al., 2017]. This framework has proven particularly effective in various domains, including games [MacGlashan et al., 2017; Christiano et al., 2017; Warnell et al., 2018], large language models [Ziegler et al., 2019; Stiennon et al., 2020; Wu et al., 2021; Nakano et al., 2021; Ouyang et al., 2022; Glaese et al., 2022; Bai et al., 2022; Ramamurthy et al., 2022; Liu et al., 2023], and robotics [Brown et al., 2019; Shin et al., 2023].

Many existing PbRL algorithms rely on online interaction with the environment, raising concerns regarding sample efficiency and safety [Christiano et al., 2017; Levine et al., 2020]. In contrast, offline PbRL operates on pre-collected datasets annotated with preference information, providing a more practical solution in scenarios where environment interaction is limited or costly [Shin et al., 2023; An et al., 2023; Kim et al., 2023; Hejna & Sadigh, 2023; Choi et al., 2024]. Despite its potential, much of the prior work in offline PbRL requires that the offline data be fully explored and often lacks sample-efficient guarantees [Zhan et al., 2023a]. The situation becomes even more challenging in scenarios where the offline data distribution only partially covers the trajectory distributions induced by some (but not all) comparator policies—that is, under partial coverage [Jin et al., 2021; Cheng et al., 2022]. In such cases, PbRL algorithms generally fail to learn a good policy with near-optimal regret in a polynomial sample complexity.

Recent efforts have sought to address the above-mentioned challenges under function approximation settings. Zhu et al. [2023] proposes a principled algorithm with sample complexity guarantees under partial coverage; however, their algorithm and theoretical guarantee are restricted to linear reward models. Zhan et al. [2023a]; Pace et al. [2024] extends this framework to the general function approximation setting by explicitly modeling the confidence sets and performing conservative learning. Nevertheless, constructing and optimizing over such confidence sets makes their algorithm computationally intractable in practice. Most recently, a concurrent work [Kang & Oh, 2025] introduces a sample-efficient approach which is able to be implemented in practice. Their algorithms either assume known transition dynamics or require fitting an extra value function that depends on the learned transition model via Bellman recursion to perform conservatism. This allows the value function to locally smooth over gaps in data coverage—if the value function is well-approximated. However, this smoothing-based mitigation strategy intrinsically requires the realizability condition on the value function and does not guarantee near-optimal regret under partial coverage [Yu et al., 2020a]. We refer the readers to Table 1 for detailed comparisons to prior works.

Table 1: Comparison of MCP and its two variants with existing methods in terms of data coverage assumptions, additional structural properties, probably approximately correct (PAC) guarantees with polynomial sample complexity, and computational tractability for practical implementation. MCP refers to our algorithm developed for general function approximation. The superscript  $\star$  indicates that the partial coverage condition is effectively refined by MCP through additional structural properties of the dynamics, resulting in improved regret bounds.

Methods	Partial Coverage	Additional Structure	PAC Guarantee	Tractable Implementation
Principled-RLHF [Zhu et al., 2023]	✓	Linear function approximation	✓	✓
FREEHAND [Zhan et al., 2023a]	✓	-	✓	✗
OPRL [Shin et al., 2023]	✗	-	✗	✓
Sim-OPRL [Pace et al., 2024]	✓	-	✓	✗
APPO [Kang & Oh, 2025]	✓	Known transition dynamics/value function realizability	✓	✓
IPL [Hejna & Sadigh, 2023]	✗	-	✗	✓
<b>MCP</b>	✓	-	✓	✓
<b>MCP-Factored<math>^\star</math></b>	✓	Factored model	✓	✓
<b>MCP-KNR<math>^\star</math></b>	✓	Kernelized nonlinear regulators	✓	✓

Motivated by the aforementioned challenges, we study the problem from a model-based learning perspective and propose an implicit way for encoding conservatism that is compatible with PbRL under general function approximation, without requiring known transition dynamics. Specifically, we relax the stringent full coverage assumption and instead assume that the offline data only needs to cover the trajectory distribution induced by the (optimal) comparator policy. We introduce **MCP**: **M**odel-based **C**onservative **P**lanning, which learns a policy through a tractable conservative learning and model-based planning procedure. The resulting policy matches the performance of any comparator policy that is covered by the offline data. MCP addresses the intractability inherent in existing methods that rely on explicitly constructing confidence sets to encode conservatism, and it avoids additional value function modeling by leveraging a purely model-based planning approach. To the best of our knowledge, MCP is the first offline PbRL algorithm that is both provably sample-efficient and computationally tractable under partial data coverage, without assuming access to the true transition dynamics. When instantiated within specialized PbRL structures, MCP further refines the concentrability coefficient in a tighter manner, leading to improved regret guarantees. In environments with factored dynamics, the regret bound of MCP scales with the number of factors and the size of their parent sets, thereby avoiding the exponential dependence on the state dimension present in non-factored models. Moreover, our analysis shows that the regret bound is adaptive to the offline data distribution and remains valid even when the state space is infinite when MCP is applied in kernelized nonlinear regulators (KNRs). Experimentally, we find that MCP achieves competitive performance compared to state-of-the-art offline PbRL methods, using real human feedback across 8 different Meta-World tasks [Yu et al., 2020b]. In addition, the conducted ablation studies demonstrate the robustness and sample efficiency of the proposed algorithm.

## 2 PRELIMINARIES

**Markov Decision Processes.** We consider a finite-horizon time-inhomogeneous Markov Decision Processes(MDP), denoted as a tuple  $M = (\mathcal{S}, \mathcal{A}, r, \{P_h\}_{h=0}^{H-1}, H, s_0)$ . Here  $\mathcal{S}$  represents the state space, and  $\mathcal{A}$  denotes the action space.  $P_h : \mathcal{S} \times \mathcal{A} \rightarrow \Delta(\mathcal{S})$  is the transition dynamics at time step  $h$ , where  $\Delta(\mathcal{S})$  denotes the set of probability distributions over states.  $r : \mathcal{T} \rightarrow [0, R_{\max}]$  is the reward

function, where  $\mathcal{T} = (\mathcal{S} \times \mathcal{A})^H$  represents the set of all trajectories of horizon length  $H$ .  $s_0$  is the initial state. We use  $r^*$  to denote the ground-truth reward function,  $\{P_h^*\}_{h=0}^{H-1}$  to denote the ground-truth transition dynamics. The agent follows a history dependent policy  $\pi := \{\pi_h\}_{h=0}^{H-1}$ , where each  $\pi_h : (\mathcal{S} \times \mathcal{A})^{h-1} \times \mathcal{S} \rightarrow \Delta(\mathcal{A})$ , specifies a distribution over actions at step  $h \in [0 : H - 1]$ , conditioned on the entire past trajectory. Let  $\Pi$  denote the set of all such history-dependent policies. Given a generic reward function  $r$  and transition dynamics  $P = \{P_h\}_{h=0}^{H-1}$ , the expected cumulative reward is defined as  $J(\pi; r, P) := \mathbb{E}_{d_P^\pi}[r(\tau)]$ , where  $d_P^\pi$  denotes the distribution over trajectories induced by executing policy  $\pi$  under transition model  $P$ . We denote  $\mathbb{E}_{d_P^\pi}[r(\tau)|s^0]$  as the expected return of trajectories starting from initial state  $s^0$ . The state-action visitation distribution at step  $h$  is defined as:  $d_h^\pi(s, a) = \mathbb{P}_P^\pi(s_h = s, a_h = a), \forall h \in [0 : H - 1]$ , where  $\mathbb{P}_P^\pi$  represents the probability distribution over trajectories generated by executing policy  $\pi$  under transition model  $P$ . Additionally, we denote the trajectory-level distribution under the ground-truth model  $P^*$  as  $d^\pi(\tau)$ .

**Offline PbRL.** Offline PbRL is a variant of reinforcement learning that deals with situations where the reward function is not directly available and instead must be inferred from human preferences over trajectory pairs. Offline PbRL focuses on learning from a dataset of trajectory pairs  $\mathcal{D} = \{(\tau^{n,0}, \tau^{n,1}, y^n)\}_{n=1}^N$ , which contains i.i.d trajectory pairs  $\tau^{n,0} = \{s_h^{n,0}, a_h^{n,0}\}_{h=0}^{H-1}, \tau^{n,1} = \{s_h^{n,1}, a_h^{n,1}\}_{h=0}^{H-1}$  sampled from reference policy  $\mu$  and binary labels  $y^n$ . Given a pair of trajectories  $(\tau^0, \tau^1)$ , a human annotator provides a binary preference label  $y \in \{0, 1\}$ , where  $y = 1$  indicates that trajectory  $\tau^1$  is preferred over  $\tau^0$ , and  $y = 0$  indicates the opposite.

To model the preference feedback between trajectories, we introduce a link function  $\Phi : \mathbb{R} \rightarrow [0, 1]$ , which is a monotonically increasing function. Given a pair of trajectories  $(\tau^0, \tau^1)$ , the preference model assumes that the probability of preferring trajectory  $\tau^1$  over  $\tau^0$  is given by:

$$\mathbb{P}(y = 1 | \tau^0, \tau^1) = \mathbb{P}(\tau^1 \text{ preferred over } \tau^0) = \Phi(r^*(\tau^1) - r^*(\tau^0))$$

One of the most commonly adopted link functions is the sigmoid function  $\sigma(x) = (1 + \exp(-x))^{-1}$ . This link function is associated with the Bradley-Terry-Luce (BTL) model [Bradley & Terry, 1952], which effectively models the relative preference between trajectories. And we define  $\kappa := (\inf_{x \in [-R_{\max}, R_{\max}]} \Phi'(x))^{-1}$  to measure the non-linearity of the link function  $\Phi$ . The goal of offline PbRL is to learn a high-performing policy  $\pi^{\text{ALG}} \in \Pi$  which satisfies the following guarantee:  $J(\pi; r^*, P^*) - J(\pi^{\text{ALG}}; r^*, P^*) \leq \epsilon$ . Here,  $\pi$  denotes a comparator policy that the learned policy aims to match or surpass in performance. For the remainder of the paper, we abuse notation by referring to  $J(\pi) - J(\pi^{\text{ALG}})$  as the regret.

**General Function Approximation.** In this work, we consider general function approximation for offline PbRL. Specifically, we model the reward and transition dynamics using a family of transition function classes  $\{\mathcal{P}_h\}_{h=0}^{H-1}$  and a reward function class  $\mathcal{R}$ . These classes are expressive enough to capture complex dynamics and reward structures through the use of linear approximators or neural networks. To quantify the complexity of the transition and reward model classes, we adopt the  $1/N$ -bracketing number metric, denoted as  $\mathcal{N}_{\mathcal{P}}(1/N)$  and  $\mathcal{N}_{\mathcal{R}}(1/N)$ , respectively [Geer, 2000].

### 3 PREFERENCE-GUIDED CONSERVATIVE PLANNING

In this section, we present a novel sample-efficient and computationally tractable offline PbRL algorithm, **Model-based Conservative Planning (MCP)**. The developed algorithm integrates model-based planning with implicitly encoded conservatism to guarantee the learned policy can compete with any (best) comparator policies within data coverage.

#### 3.1 ALGORITHM FORMULATION

We begin by presenting the motivation that underpins the design of our algorithm. The major challenge in offline PbRL is that directly performing policy learning based on the learned reward and transition models for agreement with preference feedback is inaccurate and may result in overestimation issues. To get rid of this problem, the existing works heavily rely on constructing explicit confidence sets to perform conservative learning, which is often not computationally tractable. This motivates us to develop an algorithm that alternates between encoding the conservatism into the learned reward and

162 transition models and learning the policy via a model-based planning procedure upon the worst-case  
 163 models that remain consistent with the observed preferences in offline data.

164 In MCP, we formulate the main objective to identify a policy  $\pi$  that performs favorably relative to a  
 165 reference distribution  $\mu_{ref}$ , a common choice is the distribution to induce offline data. Specifically,  
 166 we aim to maximize the performance difference between the candidate policy and the reference  
 167 distribution. This relative performance evaluation encourages policy improvement upon the reference  
 168 policy while avoiding reliance on potentially inaccurate absolute value estimates. Moreover, the  
 169 evaluation can be easily performed through a model-based planning procedure, and avoids extra value  
 170 function modeling.

$$171 \max_{\pi} J(\pi; r, \{P_h\}_{h=0}^{H-1}) - \mathbb{E}_{\tau \sim \mu_{ref}} [r(\tau)].$$

172 MCP then takes two realizable hypothesis classes for the reward and transition kernels—i.e.,  $r^* \in \mathcal{R}$   
 173 and  $P_h^* \in \mathcal{P}_h$  for all  $h \in [0 : H - 1]$ —which consist of potential data-consistent candidate models as  
 174 input, and computes the maximum likelihood models  $\hat{r}$  and  $\hat{P}_h$  using the given offline dataset  $\mathcal{D}$ . It  
 175 then formulates a minimax objective function.

$$176 \max_{\pi \in \Pi} \min_{r \in \mathcal{R}, \{P_h \in \mathcal{P}_h\}_{h=0}^{H-1}} J(\pi; r, \{P_h\}_{h=0}^{H-1}) - \mathbb{E}_{\tau \sim \mu_{ref}} [r(\tau)] + \lambda_1 \mathcal{E}_1(r; \mathcal{D}) + \lambda_2 \mathcal{E}_2(\{P_h\}_{h=0}^{H-1}; \mathcal{D}), \quad (3.1)$$

177 where the conservatism is implicitly encoded via regularizing the empirical absolute discrepancy  
 178 between the learning targets, i.e.,  $r$  and  $P_h$ , and the data-consistent models  $\hat{r}$  and  $\hat{P}_h$ :

$$179 \mathcal{E}_1(r; \mathcal{D}) = \frac{1}{N} \sum_{n=1}^N \left\| (r(\tau^{n,1}) - r(\tau^{n,0})) - (\hat{r}(\tau^{n,1}) - \hat{r}(\tau^{n,0})) \right\|, \\ 180 \mathcal{E}_2(\{P_h\}_{h=0}^{H-1}; \mathcal{D}) = \frac{1}{N} \sum_{n=1}^N \sum_{h=0}^{H-1} \sum_{i=0}^1 \left\| P_h(s_{h+1}^{n,i} | s_h^{n,i}, a_h^{n,i}) - \hat{P}_h(s_{h+1}^{n,i} | s_h^{n,i}, a_h^{n,i}) \right\|.$$

181 This minimax formulation effectively searches for a reward function  $r$  and transition model  $P_h$   
 182 within the data-consistent model class by avoiding large discrepancy from maximum likelihood  
 183 models, and then performs model-based planning using the searched conservative models. In (3.1),  
 184 the parameters  $\lambda_1$  and  $\lambda_2$  are user-specified and control the degree of conservatism encoded in  
 185 the learned models. Notably, MCP remains tractable—unlike existing approaches that encode  
 186 conservatism through the unmeasurable width of confidence sets via constrained optimization, which  
 187 often leads to intractability.

### 188 3.2 ALGORITHM IMPLEMENTATION

189 In this section, we present the details of the implementation of the MCP algorithm, building upon  
 190 the above-formulated objective function. We will establish the rigorous theoretical guarantees for  
 191 [Algorithm 1](#) later.

192 **Model Estimation (Lines 2–3).** The algorithm begins by estimating the reward model  $\hat{r}$  and the  
 193 transition model  $\hat{P}_h$  through maximizing the log-likelihood function based on the offline dataset  $\mathcal{D}$ .

194 **Conservative Planning via Relative Performance (Line 5).** In this step, MCP enforces consistency  
 195 with the offline data by regularizing the discrepancy between the learned reward and transition models  
 196 and their maximum likelihood estimators. It then implicitly encodes conservatism by performing  
 197 conservative evaluation—planning under the worst-case model based on the relative performance of  
 198 the distributions induced by  $\pi_t$  and the reference policy. This model-based evaluation avoids learning  
 199 an additional value function, improving computational efficiency.

200 **Policy Improvement (Line 6).** MCP improves the policy without explicitly searching over a policy  
 201 function class  $\Pi$ . Instead, it performs a mirror descent update, which is often utilized in online  
 202 settings [Haarnoja et al., 2018; Geist et al., 2019], which bridges the gap between the policy space and  
 203 the reward and transition model classes. As a result, the policy is no longer searched independently  
 204 of  $\mathcal{R}$  and  $\{P_h\}_{h=0}^{H-1}$ .

---

216 **Algorithm 1** Model-based Conservative Planning (MCP)

---

217 **Input:** Offline data  $\mathcal{D}$ , regularization parameters  $\lambda_1, \lambda_2$ , learning rate  $\eta$ , reference distribution  $\mu_{ref}$

218 1: Initialize policy  $\pi_1$  as the uniform policy.

219 2: **Learn reward:**  $\hat{r} = \operatorname{argmax}_{r \in \mathcal{R}} \sum_{n=1}^N \log P_r(o = o^n | \tau^{n,1}, \tau^{n,0})$ .

220 3: **Learn transition kernel:**

221 
$$\hat{P}_h = \operatorname{argmax}_{P_h \in \mathcal{P}_h} \sum_{n=1}^N \sum_{i=0}^{H-1} \log P_h(s_{h+1}^{n,i} | s_h^{n,i}, a_h^{n,i}), \forall h \in [0 : H - 1].$$

222 4: **for**  $t = 1, 2, \dots, T$  **do**

223 5:     Obtain the conservative models:  $r_t, \{P_h^t\}_{h=0}^{H-1}$ ,

224 
$$r_t, \{P_h^t\}_{h=0}^{H-1} \leftarrow \arg \min_{r \in \mathcal{R}, \{P_h \in \mathcal{P}_h\}_{h=0}^{H-1}} J(\pi_t; r, \{P_h\}_{h=0}^{H-1}) - \mathbb{E}_{\tau \sim \mu_{ref}}[r(\tau)]$$

225 
$$+ \lambda_1 \mathcal{E}_1(r; \mathcal{D}) + \lambda_2 \mathcal{E}_2(\{P_h\}_{h=0}^{H-1}; \mathcal{D}).$$

226 6:     Update  $\pi_t$  by:  $\pi_{t+1}(a|s) \propto \pi_t(a|s) \exp \left( \eta \mathbb{E}_{d_{\{P_h^t\}_{h=0}^{H-1}}^{\pi_t}}[r_t(\tau)|s, a] \right)$ .

227 7: **end for**

228 8: Output  $\pi^{\text{ALG}} := \text{MixIter}(\{\pi_t\}_{t=1}^T)$ .  $\triangleright$  mixing  $\pi_1, \dots, \pi_T$  over all iterations uniformly

---

235 **4 THEORETICAL ANALYSIS**

238 In this section, we establish the regret guarantee for the policy returned by MCP in [Algorithm 1](#) under  
 239 the partial coverage condition and general function approximation. To start with, we introduce the  
 240 notation of the concentrability coefficient to characterize the condition for the partial data coverage.  
 241 For comprehensive technical details regarding this section, please refer to [Appendix B](#).

242 **Definition 1** (Concentrability Coefficient for Reward). *For a comparator policy  $\pi$ , we define the  
 243 concentrability coefficient w.r.t. the reward function class  $\mathcal{R}$ , and a reference policy  $\mu_{ref}$ :*

$$\mathfrak{C}_R(\pi) = \sup_{r \in \mathcal{R}} \frac{\mathbb{E}_{\tau^1 \sim d^\pi, \tau^0 \sim \mu_{ref}} [\|(r(\tau^1) - r(\tau^0)) - (r^*(\tau^1) - r^*(\tau^0))\|]}{\mathbb{E}_{\tau^1 \sim \mu, \tau^0 \sim \mu} [\|(r(\tau^1) - r(\tau^0)) - (r^*(\tau^1) - r^*(\tau^0))\|]}.$$

246 **Definition 2** (Concentrability Coefficient for Transition). *For a comparator policy  $\pi$ , we define the  
 247 concentrability coefficient w.r.t. the transition function class  $\{P_h\}_{h=0}^{H-1}$ , and a reference policy  $\mu_{ref}$ :*

$$\mathfrak{C}_P(\pi) = \max_{h \in [0 : H - 1]} \sup_{P_h \in \mathcal{P}_h} \frac{\mathbb{E}_{(s,a) \sim d_h^\pi} [D_{TV}(P_h(\cdot|s, a), P_h^*(\cdot|s, a))]}{\mathbb{E}_{(s,a) \sim \mu_h} [D_{TV}(P_h(\cdot|s, a), P_h^*(\cdot|s, a))]}.$$

251 We should note that the finite concentrability coefficients implies the single-policy concentrability  
 252 that offline data covers a single good comparator policy (e.g., the optimal policy). The single-policy  
 253 concentrability is the minimum condition for the offline data coverage [[Chen & Jiang, 2022](#); [Zhan et al., 2022](#)]  
 254 in existing literature. In addition, when the reference distribution  $\mu_{ref}$  is set to  $\mu$ , the  
 255 coefficients  $\mathfrak{C}_P(\pi)$  and  $\mathfrak{C}_R(\pi)$  is upper bounded by the vanilla density ratio-based concentrability  
 256 coefficients, i.e.,  $\mathfrak{C}_P(\pi) \leq \sup_{(s,a,h)} \frac{d_h^\pi(s,a)}{\mu_h(s,a)}$  and  $\mathfrak{C}_R(\pi) \leq \sup_{\tau \in \mathcal{T}} \frac{d^\pi(\tau)}{\mu(\tau)}$ , respectively. Before we  
 257 present the main results, we impose some regular assumptions on the function classes.

258 **Assumption 1** (Realizability).  $r^* \in \mathcal{R}$  and  $P_h^* \in \mathcal{P}_h, \forall h \in [0 : H - 1]$ .

259 **Assumption 2** (Boundedness).  $0 \leq r(\tau) \leq R_{\max}, \forall r \in \mathcal{R}, \tau \in \mathcal{T}$ .

261 **Theorem 4.1.** *Suppose Assumptions 1 and 2 hold. We set the learning rate  $\eta = \sqrt{\log |\mathcal{A}| / (2R_{\max}^2 T)}$   
 262 and set the regularization coefficients  $\lambda_1 = \mathcal{O}(\mathfrak{C}_R(\pi))$  and  $\lambda_2 = \mathcal{O}(R_{\max} \sqrt{\mathfrak{C}_P(\pi) M_P})$ . Then, for  
 263 any comparator policy  $\pi \in \Pi$  with finite  $\mathfrak{C}_R(\pi)$  and  $\mathfrak{C}_P(\pi)$ , with probability at least  $1 - \delta$ , the return  
 264 policy  $\pi^{\text{ALG}}$  yielded by [Algorithm 1](#) after  $T$  iterations satisfies that*

$$J(\pi) - J(\pi^{\text{ALG}}) \leq \mathcal{O} \left( R_{\max} \sqrt{\frac{\log |\mathcal{A}|}{T}} \right) + \mathcal{O} \left( \kappa R_{\max} \mathfrak{C}_R(\pi) \sqrt{\frac{\log(\mathcal{N}_{\mathcal{R}}(1/N)/\delta)}{N}} \right) \\ + \mathcal{O} \left( R_{\max} (\mathfrak{C}_P(\pi) + M_P) H \sqrt{\frac{\log(\mathcal{N}_{\mathcal{P}}(1/N)/\delta)}{N}} \right),$$

270 where  $M_P$  is to measure the distributional shift between  $d_h^{\pi_t}$  and  $\mu_h$  under the sequence of policies  
 271 yielded in the mirror-descent trajectory of [Algorithm 1](#) for  $t = [1 : T]$  and  $h = [0 : H - 1]$ :

$$273 \quad M_P = \max_{t \in [1:T]} \max_{h \in [0:H-1]} \frac{\mathbb{E}_{(s,a) \sim d_h^{\pi_t}} [D_{TV}(P_h^t(\cdot|s,a), P_h^*(\cdot|s,a))]}{274 \quad \mathbb{E}_{(s,a) \sim \mu_h} [D_{TV}(P_h^t(\cdot|s,a), P_h^*(\cdot|s,a))]}.$$

275 Theorem 4.1 implies that the policy  $\pi^{\text{ALG}}$  is the “best-effort” policy in single-policy concentrability,  
 276 which can compete with any good comparator policy (including the optimal policy if it is covered by  
 277 offline data). In the upper bound of Theorem 4.1, the regret can be split into three parts. The last two  
 278 terms correspond to the statistical errors, which are amplified by the coverage of the offline dataset. In  
 279 general, the small  $\mathfrak{C}_P(\pi)$  and  $\mathfrak{C}_R(\pi)$  results in better statistical error guarantee. In contrast, the large  
 280 ones potentially pay high variance and statistical errors. Interestingly, we find that the distributional  
 281 shift measurement  $M_P$  influences the regret, indicating that the mirror-descent trajectory indeed  
 282 matters in [Algorithm 1](#). Note that the first term, i.e., the optimization error  $\mathcal{O}(R_{\max} \sqrt{\log |\mathcal{A}| / T})$ ,  
 283 can be reduced with the increase of the iterations  $T$ . Since the optimization error is well-controlled,  
 284 this regret guarantee is mainly determined by the last two statistical errors.

285 In many high-stakes applications, the safe policy improvement guarantees are of concern, i.e., the  
 286 return policy  $\pi^{\text{ALG}}$  is no worse than the behavior policy for generating offline data [Levine et al.,  
 287 2020]. In the following, we show that [Algorithm 1](#) guarantees the safe policy improvement.

288 **Corollary 4.2** (Safe policy improvement). *Under the conditions of Theorem 4.1, we run [Algorithm 1](#)  
 289 many iterations, i.e.,  $T$  is sufficiently large, with probability at least  $1 - \delta$ , the regret  $J(\pi_b) - J(\pi^{\text{ALG}})$   
 290 is upper bounded by*

$$292 \quad \mathcal{O} \left( R_{\max} \kappa \sqrt{\frac{\log(\mathcal{N}_{\mathcal{R}}(1/N)/\delta)}{N}} \right) + \mathcal{O} \left( R_{\max} H M_P \sqrt{\frac{\log(\mathcal{N}_{\mathcal{P}}(1/N)/\delta)}{N}} \right).$$

295 Next, we study the sample complexity of MCP and demonstrate that our algorithm achieves improved  
 296 performance in comparison to prior works.

297 **Corollary 4.3** (Sample complexity). *Under the conditions of Theorem 4.1, the  $\pi^{\text{ALG}}$  in [Algorithm 1](#)  
 298 satisfies  $J(\pi) - J(\pi^{\text{ALG}}) \leq R_{\max} \varepsilon$  with probability at least  $\geq 1 - \delta$ , if the sample size attains*

$$300 \quad \mathcal{O} \left( \frac{\kappa^2 \mathfrak{C}_R^2(\pi) \log(\mathcal{N}_{\mathcal{R}}(1/N)/\delta)}{\epsilon^2} + \frac{H^2 (\mathfrak{C}_P(\pi) + M_P)^2 \log(\mathcal{N}_{\mathcal{P}}(1/N)/\delta)}{\epsilon^2} \right).$$

302 In comparison to some prior works, Kang & Oh [2025] requires sample complexity:

$$304 \quad \mathcal{O} \left( \max \left\{ \frac{R_{\max}^4 H^5 \log |\mathcal{A}| \log(H|\mathcal{F}|/\delta)}{\epsilon^4}, \frac{R_{\max}^2 H^2 \log(H|\mathcal{P}|/\delta)}{\epsilon^2} \right\} + \frac{\mathfrak{C}_{TR}^2 \kappa^2 H \log(|\mathcal{R}|/\delta)}{\epsilon^2} \right),$$

306 where  $|\cdot|$  denotes the cardinality of the value function class,  $\mathfrak{C}_{TR} = \sup_{\tau \in \mathcal{T}} \frac{d^{\pi}(\tau)}{\mu(\tau)}$ . This implies that  
 307 the results in Kang & Oh [2025] are restricted to finite classes, but we can handle the infinite classes.  
 308 Moreover, the bound in Kang & Oh [2025] is dependent on an extra model class  $\mathcal{F}$ , and we avoid this  
 309 additional complexity via leveraging a relative-performance model-based planning procedure. Also,  
 310 the MCP is more sample efficient, i.e.,  $\mathcal{O}(\epsilon^{-2})$  vs  $\mathcal{O}(\epsilon^{-4})$ . In comparison to the work Zhan et al.  
 311 [2023a], they attain a sample complexity of the same order as ours, but it requires explicitly solving  
 312 for the confidence set radius, which is computationally intractable. In contrast, MCP achieves both  
 313 statistical efficiency and computational efficiency by avoiding constructing explicit confidence sets.

## 315 5 SPECIALIZED STRUCTURES ON DYNAMICS

317 In the previous section, the results were established for general function approximation. In the  
 318 following, we consider structured dynamics and show that MCP can exploit additional structural  
 319 properties to refine the model-based concentrability coefficients into more interpretable and natural  
 320 quantities, leading to improved regret bounds. Specifically, we analyze two representative examples:  
 321 (1) Kernelized nonlinear regulators (KNRs [Kakade et al., 2020]), which capture smooth nonlinear  
 322 dynamics common in control and robotics, and (2) Factored model [Kearns & Koller, 1999], particu-  
 323 larly effective in dealing with high-dimensional environments, e.g., via conditional independence.  
 For comprehensive technical details regarding this section, please refer to Appendix D and E.

324  
325

## 5.1 KERNELIZED NONLINEAR REGULATORS

326  
327  
328  
329  
330  
331  
332  
333  
334

A kernelized nonlinear regulator is a model that assumes the next state is a linear transformation of a nonlinear embedding of the current state and action, corrupted by Gaussian noise [Kakade et al., 2020]. Formally, the transition model is given by:  $s' = W^* \phi(s, a) + \epsilon$ ,  $\epsilon \sim \mathcal{N}(0, \zeta^2 I)$ , where  $\zeta \in \mathbb{R}$ ,  $s \in \mathbb{R}^{d'}$ ,  $a \in \mathbb{R}^{d_a}$ , and  $\phi : \mathcal{S} \times \mathcal{A} \rightarrow \mathbb{R}^d$  is a nonlinear feature mapping. The true model is parameterized by the unknown weight matrix  $W^*$ , and the corresponding class of models is indexed by  $W$ , so that each candidate model is denoted by  $P_W$ . To establish the regret guarantee for MCP in the KNRs setting, we define a new concentrability coefficient that takes advantage of the structure of KNRs. Let  $\Sigma_\pi = \mathbb{E}_{(s, a) \sim d^\pi} [\phi(s, a) \phi(s, a)^\top]$ ,  $\Sigma_\mu = \mathbb{E}_{(s, a) \sim \mu} [\phi(s, a) \phi(s, a)^\top]$  and  $\Sigma_n = \sum_{i=1}^n \phi(s_i, a_i) \phi(s_i, a_i)^\top + \lambda I$ . We define the relative condition number as:

335  
336  
337

$$\mathfrak{C}_P^K(\pi) = \sup_{x \in \mathbb{R}^d} \left( \frac{x^\top \Sigma_\pi x}{x^\top \Sigma_\mu x} \right).$$

338  
339  
340  
341  
342

We should note that  $D_{TV}(P_W(\cdot|s, a), P_{W^*}(\cdot|s, a)) = c(\|W - W^*\|_2)$  [Devroye et al., 2018], where  $c$  is a universal constant. It is easy to show that  $\mathfrak{C}_P(\pi)$  is upper-bounded by the relative condition number  $\mathfrak{C}_P^K(\pi)$ . We now tailor Algorithm 1 to the KNR setting. We need to modify the maximum likelihood estimator of the transition model to a kernelized nonlinear regularized variant, i.e.,

343

$$\widehat{W} = \arg \min_{W \in \mathbb{R}^{d' \times d}} \mathbb{E}_{\mathcal{D}} [\|W \phi(s, a) - s'\|_2^2] + \lambda \|W\|_F^2,$$

344  
345  
346  
347

where  $\|W\|_F$  is the Frobenius norm of  $W$ . Now we are prepared to state the regret bound for MCP in the KNR setting.

348  
349  
350  
351  
352

**Theorem 5.1** (PAC Bound in KNRs). *Under the conditions of Theorem 4.1, suppose  $\|\phi(s, a)\|_2 \leq 1$ ,  $\|W\|_2^2 = \mathcal{O}(1)$ ,  $\zeta^2 = \mathcal{O}(1)$ ,  $\lambda = \mathcal{O}(1)$ , and  $\|W\|_F \leq c_W$  hold. We set  $\lambda_1 = \mathcal{O}(\mathfrak{C}_R(\pi))$  and  $\lambda_2 = \mathcal{O}(R_{\max} \sqrt{\mathfrak{C}_P(\pi) M_P^K})$ . For any good comparator policy  $\pi$ , with probability at least  $1 - \delta$ , the yielded  $\pi^{\text{ALG}}$  by the KNR-modified Algorithm 1 satisfies that*

353  
354  
355  
356  
357  
358

$$\begin{aligned} J(\pi) - J(\pi^{\text{ALG}}) &\leq \mathcal{O} \left( R_{\max} \sqrt{\frac{\log |\mathcal{A}|}{T}} \right) + \mathcal{O} \left( \kappa R_{\max} \mathfrak{C}_R(\pi) \sqrt{\frac{\log(\mathbb{N}_{\mathcal{R}}/\delta)}{N}} \right) \\ &\quad + \mathcal{O} \left( R_{\max} (\mathfrak{C}_P^K(\pi) + M_P^K) H \xi \left( \lambda_{\Sigma_n^{-1}} \sqrt{\frac{\log(H\mathbb{N}_{\mathcal{P}}/\delta)}{N}} + \Gamma(N, \delta) \right) \right), \end{aligned}$$

359  
360  
361  
362  
363

where the coefficients  $\lambda_{\Sigma_n^{-1}} = \sqrt{\lambda_{\max}(\Sigma_n^{-1})}$ ,  $M_P^K = \max_{t \in [1:T]} \sup_{x \in \mathbb{R}^d} \left( \frac{x^\top \Sigma_{\pi_t} x}{x^\top \Sigma_\mu x} \right)$ ,  $\Gamma(N, \delta) = \sqrt{\text{rank}(\Sigma_\mu) \{\log(\exp(\text{rank}(\Sigma_\mu)/\delta))\}/N}$ , and  $\xi = \|W^*\|_2 + d' \min(d, \text{rank}(\Sigma_\mu))(\text{rank}(\Sigma_\mu) + \log(1/\delta)) \log(1 + N)$ . The complexity of the function class in the KNR settings is characterized as  $\mathbb{N}_{\mathcal{P}} = \text{rank}(\Sigma_\mu) d' \log(1 + 2c_W N)$ ,  $\mathbb{N}_{\mathcal{R}} = d' \log(1 + 2N)$ .

364  
365  
366  
367  
368  
369

In comparison to Theorem 4.1, the main contribution of the modified algorithm MCP-KNR is on exploiting the KNR structures and improving the regret bound. In particular, the appearance of  $\text{rank}(\Sigma_\mu)$  in the bound, instead of the feature dimension  $d$ , ensures that the result adapts to the complexity of the data distribution. Notably, the bound holds even when  $d$  is infinite, provided that the data concentrates on a low-dimensional subspace.

370  
371

## 5.2 FACTORED MODELS

372  
373  
374  
375  
376  
377

Factored models provide a compact representation for large-scale MDPs by exploiting structure in the state space [Osband & Van Roy, 2014]. Let  $d \in \mathbb{N}^+$  and  $\mathcal{B}$  be a small finite set. Rather than modeling the full transition probability over all state variables, they decompose the state  $s \in \mathbb{R}^d$  into components and assume that each component  $s[i]$  of the next state depends only on a small set of parent variables  $\mathcal{P}_i \subseteq [1 : d]$ . This yields a transition function of the form  $P(s'|s, a) = \prod_{i=1}^d P_i(s'[i]|s[\mathcal{P}_i], a)$ , significantly reducing the number of parameters compared to the unfactored case. This factorization drastically reduces the model complexity: the number of parameters for the

378 transition function becomes  $L_p := \sum_{i=1}^d |\mathcal{A}| \cdot |\mathcal{B}|^{1+|\mathcal{P}_i|}$ , as opposed to the exponential size  $\mathcal{O}(\mathcal{B}^d)$   
 379 in the fully connected case, enabling more sample-efficient learning from limited data. To adapt  
 380 [Algorithm 1](#) to this structured setting and formulate a new algorithm—MCP-Factored—we modify  
 381 the maximum likelihood estimation step by estimating each transition component  $P_i$  separately  
 382 via  $\widehat{P}_i = \arg \max_P \mathbb{E}_{\mathcal{D}} [\log P(s'[i]|s[\mathcal{P}_i], a)]$ , and reconstruct the full transition model as  $\widehat{P} =$   
 383  $\prod_{i=1}^d \widehat{P}_i$ . Before we present the regret guarantee for MCP-Factored, let us define a new concentrability  
 384 coefficient. Instead of using the density ratio over the full state space, we measure it locally for each  
 385 factor of the transition model. Specifically, for any comparator policy  $\pi$ , we define  
 386

$$\mathfrak{C}_P^F(\pi) = \max_{i \in [1:d]} \mathbb{E}_{(s,a) \sim \mu} \left[ \left( \frac{d^\pi(s[\mathcal{P}_i], a)}{\mu(s[\mathcal{P}_i], a)} \right)^2 \right].$$

390 We should note that this factored concentrability coefficient  $\mathfrak{C}_P^F(\pi)$  relaxes the density ratio-based  
 391 single-policy concentrability coefficient, i.e.,  $\mathfrak{C}_P^F(\pi) \leq \sup_{(s,a,h)} \frac{d_h^\pi(s,a)}{\mu_h(s,a)}$ . We now present the regret  
 392 bound for the MCP-Factored algorithm.

393 **Theorem 5.2** (PAC Bound in Factored Models). *Under the conditions of Theorem 4.1, we set  
 394  $\lambda_1 = \mathcal{O}(\mathfrak{C}_R(\pi))$ ,  $\lambda_2 = \mathcal{O}(R_{\max} \sqrt{\mathfrak{C}_P(\pi) M_P^F})$ . For any good comparator policy  $\pi$ , with probability  
 395 at least  $1 - \delta$ , after sufficiently large number of iterations, the yielded  $\pi^{\text{ALG}}$  by the Factored-modified  
 396 [Algorithm 1](#) satisfies that the regret  $J(\pi_b) - J(\pi^{\text{ALG}})$  is upper bounded by*

$$400 \mathcal{O} \left( \kappa \mathfrak{C}_R(\pi) R_{\max} \sqrt{\frac{\log(rL_r/\delta)}{N}} \right) + \mathcal{O} \left( (\mathfrak{C}_P^F(\pi) + M_P^F) HR_{\max} \sqrt{\frac{dL_p \log(L_p N d/\delta)}{N}} \right).$$

401 Here,  $M_P^F = \max_{t \in [1:T]} \max_{i \in [1:d]} \mathbb{E}_{(s,a) \sim \mu} \left[ \left( \frac{d^\pi(s[\mathcal{P}_i], a)}{\mu(s[\mathcal{P}_i], a)} \right)^2 \right]$  and  $L_r = \sum_{i=1}^d |\mathcal{A}| \cdot |\mathcal{B}|^{1+|\mathcal{U}_i^a|}$ , where  $\mathcal{U}_i^a$   
 402 denotes the effective dimension of the state variables on which the reward model depends.

403 The key observation in Theorem 5.2 is as follows: Instead of depending on the full state space as  
 404 in the results for general function approximation, MCP-Factored leverages the structure of factored  
 405 models and therefore the PAC bound scales with the number of factors and the sizes of their parent  
 406 sets, summarized by the complexity term  $L_p$  and  $L_r$ . This avoids the exponential dependence on the  
 407 state dimension  $d$  seen in the non-factored models.

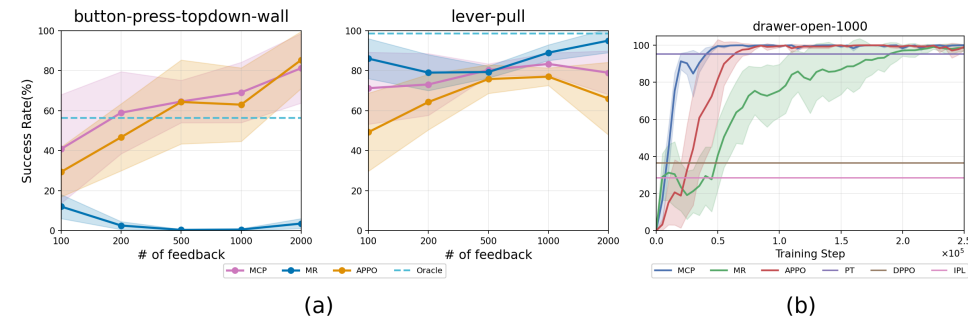
## 6 EXPERIMENTS

414 **Benchmarks and Evaluation.** We evaluate the algorithmic performance of MCP on Meta-World  
 415 benchmark datasets with preference feedback [Yu et al., 2020a; Kang & Oh, 2025]. We refer the  
 416 readers to the Appendix F for details of benchmarks. In Table 2, we summarize the success rates  
 417 of MCP and several competitive baselines, including Oracle (IQL [Kostrikov et al., 2021] trained  
 418 on ground-truth explicit rewards), MR [Kim et al., 2023], PT [Kim et al., 2023], DPPO [An et al.,  
 419 2023], IPL [Hejna & Sadigh, 2023], and APPPO [Kang & Oh, 2025]. Most notably, MCP achieves the  
 420 best mean performance for 8 tasks with varying sizes of preference samples. Another noteworthy  
 421 observation is that MCP overwhelmingly outperforms APPPO for the majority of the tasks. Although  
 422 MCP and APPPO are all model-based algorithms, APPPO leverages the extra value function modeling  
 423 to locally smooth over gaps in data coverage. This smoothing-based mitigation is still not sufficient to  
 424 guarantee robustness in poor data coverage scenarios. Due to page limits, we provide the additional  
 425 empirical results and implementation details in Appendix G.

426 **Effect of Dataset Size.** To evaluate the performance of MCP under varying amounts of preference  
 427 data—especially in small-data regimes—we train the model using different numbers of preferences,  
 428 ranging from 100 to 2000, as shown in Figure 1(a). Notably, even with extremely limited data, i.e.,  
 429  $N = 100$ , MCP maintains a relatively high success rate, highlighting its potential for applications  
 430 with small preference datasets, such as those in medicine and finance.

432 Table 2: Below reports the success rates on the Meta-World medium-replay benchmark using 500  
 433 and 1000 preference-based feedback samples, averaged across three distinct random seeds. Baseline  
 434 results are from the respective papers. Note that the top two algorithms in each experiment are  
 435 highlighted in bold, with the best-performing algorithm additionally shaded in light gray.

Dataset & Methods	Oracle	MR	PT	DPPO	IPL	APPO	MCP
BPT-500	88.33 $\pm$ 4.76	10.08 $\pm$ 7.57	22.87 $\pm$ 9.06	3.93 $\pm$ 4.34	34.73 $\pm$ 13.9	<b>53.52</b> $\pm$ 13.9	<b>56.00</b> $\pm$ 14.1
box-close-500	93.40 $\pm$ 3.10	<b>29.12</b> $\pm$ 11.3	0.33 $\pm$ 1.16	10.20 $\pm$ 11.5	5.93 $\pm$ 5.81	<b>18.24</b> $\pm$ 15.60	7.20 $\pm$ 3.87
sweep-500	98.33 $\pm$ 1.87	<b>86.96</b> $\pm$ 6.93	<b>43.07</b> $\pm$ 24.6	10.47 $\pm$ 15.8	27.20 $\pm$ 23.8	26.80 $\pm$ 5.32	11.47 $\pm$ 9.93
BPT-wall-500	56.27 $\pm$ 6.32	0.32 $\pm$ 0.30	0.87 $\pm$ 1.43	0.80 $\pm$ 1.51	8.93 $\pm$ 9.84	<b>64.32</b> $\pm$ 21.0	<b>64.53</b> $\pm$ 10.6
dial-turn-500	75.40 $\pm$ 5.47	<b>61.44</b> $\pm$ 6.08	68.67 $\pm$ 12.4	26.67 $\pm$ 22.2	31.53 $\pm$ 12.5	<b>80.96</b> $\pm$ 4.49	38.67 $\pm$ 7.65
sweep-into-500	78.80 $\pm$ 7.96	28.40 $\pm$ 5.47	20.53 $\pm$ 8.26	23.07 $\pm$ 7.02	<b>32.20</b> $\pm$ 7.35	24.08 $\pm$ 5.91	<b>33.07</b> $\pm$ 4.71
drawer-open-500	100.00 $\pm$ 0.00	<b>98.00</b> $\pm$ 2.32	88.73 $\pm$ 11.6	35.93 $\pm$ 11.2	19.00 $\pm$ 13.6	87.68 $\pm$ 10.0	<b>98.67</b> $\pm$ 0.94
lever-pull-500	98.47 $\pm$ 1.77	79.28 $\pm$ 2.95	<b>82.40</b> $\pm$ 22.7	10.13 $\pm$ 12.2	31.20 $\pm$ 18.5	75.76 $\pm$ 7.17	<b>80.27</b> $\pm$ 3.10
<i>Average Rank -500</i>	—	3.000	3.500	5.250	4.000	2.875	<b>2.375</b>
BPT-1000	88.33 $\pm$ 4.76	8.48 $\pm$ 5.80	18.27 $\pm$ 10.6	3.20 $\pm$ 3.04	36.67 $\pm$ 17.4	<b>59.04</b> $\pm$ 19.0	<b>62.93</b> $\pm$ 17.8
box-close-1000	93.40 $\pm$ 3.10	<b>27.04</b> $\pm$ 14.5	2.27 $\pm$ 2.86	9.33 $\pm$ 6.90	6.73 $\pm$ 8.41	<b>34.24</b> $\pm$ 18.5	10.53 $\pm$ 5.78
sweep-1000	98.33 $\pm$ 1.87	<b>87.52</b> $\pm$ 7.87	29.13 $\pm$ 14.8	8.73 $\pm$ 16.4	<b>38.33</b> $\pm$ 24.9	17.36 $\pm$ 12.4	20.80 $\pm$ 11.91
BPT-wall-1000	56.27 $\pm$ 6.32	0.48 $\pm$ 0.47	2.13 $\pm$ 2.96	0.27 $\pm$ 0.85	14.07 $\pm$ 11.5	<b>62.96</b> $\pm$ 18.4	<b>69.73</b> $\pm$ 15.1
dial-turn-1000	75.40 $\pm$ 5.47	<b>69.44</b> $\pm$ 7.00	68.80 $\pm$ 5.50	36.40 $\pm$ 21.9	43.93 $\pm$ 13.4	<b>81.44</b> $\pm$ 6.73	48.40 $\pm$ 5.82
sweep-into-1000	78.80 $\pm$ 7.96	26.00 $\pm$ 5.53	20.27 $\pm$ 7.84	23.33 $\pm$ 7.30	<b>30.40</b> $\pm$ 7.74	18.16 $\pm$ 11.1	<b>34.13</b> $\pm$ 3.27
drawer-open-1000	100.00 $\pm$ 0.00	98.40 $\pm$ 2.82	95.32 $\pm$ 4.26	36.47 $\pm$ 7.90	28.53 $\pm$ 18.4	<b>98.56</b> $\pm$ 2.68	<b>99.07</b> $\pm$ 0.38
lever-pull-1000	98.47 $\pm$ 1.77	<b>88.96</b> $\pm$ 3.28	72.93 $\pm$ 10.2	8.53 $\pm$ 9.96	40.40 $\pm$ 17.4	76.96 $\pm$ 4.40	<b>83.33</b> $\pm$ 5.51
<i>Average Rank -1000</i>	—	2.750	4.125	5.375	3.875	2.750	<b>2.125</b>
<b>Average Rank</b>	—	2.875	3.812	5.312	3.938	2.813	<b>2.250</b>

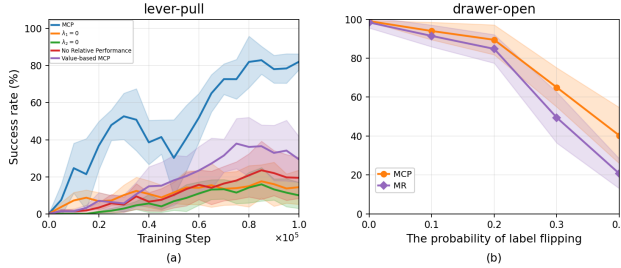


468 Figure 1: (a) Model performance varying with dataset size, i.e., the number of preference feedback,  
 469 ranging from 100 to 2000. (b) Training curves for drawer-open with 1000 preferences. We evaluate  
 470 the results over three seeds, and the horizontal lines indicate the baseline performance summarized in  
 471 Table 2.

472 **Training Dynamics.** We study the training dynamics of MCP for drawer-open with 1000 preferences  
 473 in Figure 1(b). We evaluate the training performance every 5000 steps. Figure 1(b) demonstrates that  
 474 MCP achieves comparable performance with state-of-the-art baselines in the task. Also, it shows that  
 475 MCP maintains stability in the policy improvement process, especially after sufficient training steps.

476 **Ablation Study.** We investigate the contribution of each design component of MCP on the lever-  
 477 pull task with 1000 preferences in Figure 2(a). The figure compares the full MCP algorithm with  
 478 several variants obtained by removing the reward regularization ( $\lambda_1 = 0$ ), removing the transition  
 479 regularization ( $\lambda_2 = 0$ ), dropping the relative performance term (“No Relative Performance”), and  
 480 replacing the model-based planner with a value-based variant (“Value-based MCP”). We evaluate  
 481 the success rate every 5000 training steps and report the mean and standard deviation over three  
 482 seeds. Figure 2(a) shows that full MCP rapidly reaches a high success rate and clearly outperforms  
 483 all ablated variants. In particular, the variants without reward or transition regularization make little  
 484 progress, indicating that the conservative modeling terms are essential for avoiding over-optimistic  
 485 and unstable policies. The “No Relative Performance” variant exhibits large variability and unstable  
 486 learning, which is consistent with the lack of the safe policy improvement guarantee provided by

486 the relative-performance objective. The “Value-based MCP” variant improves in the early stage  
 487 but then degrades, suggesting that relying solely on value-based updates introduces significant bias  
 488 from model errors. Overall, these results confirm that all four model components are crucial for  
 489 guaranteeing the consistent policy improvement.



500  
 501 Figure 2: (a) Ablation of MCP design components on lever-pull-1000. (b) Robustness to label noise  
 502 on drawer-open-1000 (performance vs. label-flipping probability).

503 **Robustness to Label Noise.** We further examine the robustness of MCP to noisy preference labels  
 504 on the drawer-open task in Figure 2(b). Starting from a dataset with 1000 preferences, we introduce  
 505 synthetic noise by independently flipping each pairwise label with probability  $p$  and vary  $p$  over  
 506 several levels. The figure reports the resulting success rates of MCP and MR, averaged over three  
 507 seeds. As the label-flipping probability increases, the performance of both methods degrades, but  
 508 MCP consistently maintains higher success rates and exhibits a slower decay than MR. This result  
 509 demonstrates that the conservative design of MCP provides improved robustness to label noise.

510 Table 3: Sensitivity of MCP to regularization hyperparameters on *drawer-open-1000* and *sweep-into-1000*.

$\lambda_1$	1e-1	3e-1	1	3	1e1
drawer-open-1000	94.8 $\pm$ 3.85	97.60 $\pm$ 2.33	99.07 $\pm$ 0.38	94.53 $\pm$ 4.03	86.27 $\pm$ 10.31
sweep-into-1000	32.4 $\pm$ 5.85	34.13 $\pm$ 3.27	30.67 $\pm$ 4.71	24.0 $\pm$ 9.27	19.87 $\pm$ 7.92
$\lambda_2$	3e-3	1e-2	3e-2	1e-1	1
drawer-open-1000	90.93 $\pm$ 7.30	95.47 $\pm$ 4.10	99.07 $\pm$ 0.38	89.60 $\pm$ 9.53	80.13 $\pm$ 15.19
sweep-into-1000	20.8 $\pm$ 10.32	23.6 $\pm$ 5.85	28.27 $\pm$ 7.08	34.13 $\pm$ 3.27	25.73 $\pm$ 6.15

519 **Hyperparameter sensitivity.** We conduct a hyperparameter sensitivity analysis for the regularization  
 520 weights  $\lambda_1, \lambda_2$  on the *drawer-open-1000* and *sweep-into-1000* tasks over three seeds. As shown  
 521 in Table 3, across several orders of magnitude for each parameter, the success rate of MCP changes  
 522 only mildly, indicating that our method is not highly sensitive to the exact choice of  $\lambda_1, \lambda_2$ .

## 524 7 DISCUSSION

526 In this work, we present the first provably sample-efficient and computationally tractable offline PbRL  
 527 under partial data coverage without known dynamics. The developed algorithm implicitly encodes  
 528 the conservatism into a relative performance model-based planning procedure, and guarantees the  
 529 algorithmic traceability. The learned policy is able to compete with any policies within the data  
 530 coverage, making it robust even in scenarios with poor data coverage. We further extend and refine  
 531 the theoretical results with general function approximation under specialized dynamic structures.  
 532 As a potential research direction, it is interesting to extend the Bradley–Terry–Luce framework for  
 533 modeling human preferences by incorporating alternative preference models, e.g., Thurstone model.

## 535 REFERENCES

537 Riad Akroud, Marc Schoenauer, and Michèle Sebag. April: Active preference learning-based  
 538 reinforcement learning. In *Machine Learning and Knowledge Discovery in Databases: European  
 539 Conference, ECML PKDD 2012, Bristol, UK, September 24-28, 2012. Proceedings, Part II* 23, pp.  
 116–131. Springer, 2012.

540 Gaon An, Junhyeok Lee, Xingdong Zuo, Norio Kosaka, Kyung-Min Kim, and Hyun Oh Song. Direct  
 541 preference-based policy optimization without reward modeling. *Advances in Neural Information  
 542 Processing Systems*, 36:70247–70266, 2023.

543

544 Yuntao Bai, Andy Jones, Kamal Ndousse, Amanda Askell, Anna Chen, Nova DasSarma, Dawn Drain,  
 545 Stanislav Fort, Deep Ganguli, Tom Henighan, et al. Training a helpful and harmless assistant with  
 546 reinforcement learning from human feedback. *arXiv preprint arXiv:2204.05862*, 2022.

547

548 Ralph Allan Bradley and Milton E Terry. Rank analysis of incomplete block designs: I. the method  
 549 of paired comparisons. *Biometrika*, 39(3/4):324–345, 1952.

550

551 Daniel Brown, Wonjoon Goo, Prabhat Nagarajan, and Scott Niekum. Extrapolating beyond sub-  
 552 optimal demonstrations via inverse reinforcement learning from observations. In *International  
 553 conference on machine learning*, pp. 783–792. PMLR, 2019.

554

555 Daniel Brown, Russell Coleman, Ravi Srinivasan, and Scott Niekum. Safe imitation learning via fast  
 556 bayesian reward inference from preferences. In *International Conference on Machine Learning*,  
 557 pp. 1165–1177. PMLR, 2020.

558

559 Jonathan Chang, Masatoshi Uehara, Dhruv Sreenivas, Rahul Kidambi, and Wen Sun. Mitigating  
 560 covariate shift in imitation learning via offline data with partial coverage. *Advances in Neural  
 561 Information Processing Systems*, 34:965–979, 2021.

562

563 Jinglin Chen and Nan Jiang. Offline reinforcement learning under value and density-ratio realizability:  
 564 the power of gaps. In *Uncertainty in Artificial Intelligence*, pp. 378–388. PMLR, 2022.

565

566 Xiaoyu Chen, Han Zhong, Zhuoran Yang, Zhaoran Wang, and Liwei Wang. Human-in-the-loop:  
 567 Provably efficient preference-based reinforcement learning with general function approximation.  
 568 In *International Conference on Machine Learning*, pp. 3773–3793. PMLR, 2022.

569

570 Ching-An Cheng, Tengyang Xie, Nan Jiang, and Alekh Agarwal. Adversarially trained actor critic for  
 571 offline reinforcement learning. In *International Conference on Machine Learning*, pp. 3852–3878.  
 572 PMLR, 2022.

573

574 Heewoong Choi, Sangwon Jung, Hongjoon Ahn, and Taesup Moon. Listwise reward estimation for  
 575 offline preference-based reinforcement learning. *arXiv preprint arXiv:2408.04190*, 2024.

576

577 Paul F Christiano, Jan Leike, Tom Brown, Miljan Martic, Shane Legg, and Dario  
 578 Amodei. Deep reinforcement learning from human preferences. In I. Guyon, U. Von  
 579 Luxburg, S. Bengio, H. Wallach, R. Fergus, S. Vishwanathan, and R. Garnett (eds.), *Ad-  
 580 vances in Neural Information Processing Systems*, volume 30. Curran Associates, Inc.,  
 581 2017. URL [https://proceedings.neurips.cc/paper\\_files/paper/2017/  
 582 file/d5e2c0adad503c91f91df240d0cd4e49-Paper.pdf](https://proceedings.neurips.cc/paper_files/paper/2017/file/d5e2c0adad503c91f91df240d0cd4e49-Paper.pdf).

583

584 Luc Devroye, Abbas Mehrabian, and Tommy Reddad. The total variation distance between high-  
 585 dimensional gaussians with the same mean. *arXiv preprint arXiv:1810.08693*, 2018.

586

587 Scott Fujimoto and Shixiang Shane Gu. A minimalist approach to offline reinforcement learning.  
 588 *Advances in neural information processing systems*, 34:20132–20145, 2021.

589

590 Sara A Geer. *Empirical Processes in M-estimation*, volume 6. Cambridge university press, 2000.

591

592 Matthieu Geist, Bruno Scherrer, and Olivier Pietquin. A theory of regularized markov decision  
 593 processes. In *International conference on machine learning*, pp. 2160–2169. PMLR, 2019.

594

595 Amelia Glaese, Nat McAleese, Maja Trębacz, John Aslanides, Vlad Firoiu, Timo Ewalds, Maribeth  
 596 Rauh, Laura Weidinger, Martin Chadwick, Phoebe Thacker, et al. Improving alignment of dialogue  
 597 agents via targeted human judgements. *arXiv preprint arXiv:2209.14375*, 2022.

598

599 Tuomas Haarnoja, Aurick Zhou, Pieter Abbeel, and Sergey Levine. Soft actor-critic: Off-policy  
 600 maximum entropy deep reinforcement learning with a stochastic actor. In *International conference  
 601 on machine learning*, pp. 1861–1870. Pmlr, 2018.

594 Joey Hejna and Dorsa Sadigh. Inverse preference learning: Preference-based rl without a reward  
 595 function. *Advances in Neural Information Processing Systems*, 36:18806–18827, 2023.  
 596

597 Donald Joseph Hejna III and Dorsa Sadigh. Few-shot preference learning for human-in-the-loop rl.  
 598 In *Conference on Robot Learning*, pp. 2014–2025. PMLR, 2023.

599 Ying Jin, Zhuoran Yang, and Zhaoran Wang. Is pessimism provably efficient for offline rl? In  
 600 *International Conference on Machine Learning*, pp. 5084–5096. PMLR, 2021.  
 601

602 Sham Kakade and John Langford. Approximately optimal approximate reinforcement learning. In  
 603 *Proceedings of the nineteenth international conference on machine learning*, pp. 267–274, 2002.

604 Sham Kakade, Akshay Krishnamurthy, Kendall Lowrey, Motoya Ohnishi, and Wen Sun. Information  
 605 theoretic regret bounds for online nonlinear control. *Advances in Neural Information Processing  
 606 Systems*, 33:15312–15325, 2020.  
 607

608 Hyungkyu Kang and Min-hwan Oh. Adversarial policy optimization for offline preference-based  
 609 reinforcement learning. *arXiv preprint arXiv:2503.05306*, 2025.

610 Michael Kearns and Daphne Koller. Efficient reinforcement learning in factored mdps. In *Proceedings  
 611 of the 16th International Joint Conference on Artificial Intelligence - Volume 2*, IJCAI'99, pp.  
 612 740–747, San Francisco, CA, USA, 1999. Morgan Kaufmann Publishers Inc.  
 613

614 Rahul Kidambi, Aravind Rajeswaran, Praneeth Netrapalli, and Thorsten Joachims. Morel: Model-  
 615 based offline reinforcement learning. *Advances in neural information processing systems*, 33:  
 616 21810–21823, 2020.

617 Changyeon Kim, Jongjin Park, Jinwoo Shin, Honglak Lee, Pieter Abbeel, and Kimin Lee. Pref-  
 618 erence transformer: Modeling human preferences using transformers for rl. *arXiv preprint  
 619 arXiv:2303.00957*, 2023.  
 620

621 Diederik P Kingma and Jimmy Ba. Adam: A method for stochastic optimization. *arXiv preprint  
 622 arXiv:1412.6980*, 2014.

623 Ilya Kostrikov, Ashvin Nair, and Sergey Levine. Offline reinforcement learning with implicit  
 624 q-learning. *arXiv preprint arXiv:2110.06169*, 2021.

625 Aviral Kumar, Aurick Zhou, George Tucker, and Sergey Levine. Conservative q-learning for offline  
 626 reinforcement learning. *Advances in neural information processing systems*, 33:1179–1191, 2020.  
 627

628 Kimin Lee, Laura Smith, and Pieter Abbeel. Pebble: Feedback-efficient interactive reinforcement  
 629 learning via relabeling experience and unsupervised pre-training. *arXiv preprint arXiv:2106.05091*,  
 630 2021.  
 631

632 Sergey Levine, Aviral Kumar, George Tucker, and Justin Fu. Offline reinforcement learning: Tutorial,  
 633 review, and perspectives on open problems. *arXiv preprint arXiv:2005.01643*, 2020.

634 Gen Li, Laixi Shi, Yuxin Chen, Yuejie Chi, and Yuting Wei. Settling the sample complexity of  
 635 model-based offline reinforcement learning. *The Annals of Statistics*, 52(1):233–260, 2024.  
 636

637 David Lindner, Matteo Turchetta, Sebastian Tschiatschek, Kamil Ciosek, and Andreas Krause.  
 638 Information directed reward learning for reinforcement learning. *Advances in Neural Information  
 639 Processing Systems*, 34:3850–3862, 2021.  
 640

641 Hao Liu, Carmelo Sferrazza, and Pieter Abbeel. Chain of hindsight aligns language models with  
 642 feedback. *arXiv preprint arXiv:2302.02676*, 2023.

643 Yao Liu, Adith Swaminathan, Alekh Agarwal, and Emma Brunskill. Provably good batch off-policy  
 644 reinforcement learning without great exploration. *Advances in neural information processing  
 645 systems*, 33:1264–1274, 2020.

646 Ilya Loshchilov and Frank Hutter. Decoupled weight decay regularization. *arXiv preprint  
 647 arXiv:1711.05101*, 2017.

648 James MacGlashan, Mark K. Ho, Robert Loftin, Bei Peng, Guan Wang, David L. Roberts, Matthew E.  
 649 Taylor, and Michael L. Littman. Interactive learning from policy-dependent human feedback. In  
 650 Doina Precup and Yee Whye Teh (eds.), *Proceedings of the 34th International Conference on Ma-  
 chine Learning*, volume 70 of *Proceedings of Machine Learning Research*, pp. 2285–2294. PMLR,  
 651 06–11 Aug 2017. URL <https://proceedings.mlr.press/v70/macglashan17a.html>.

652

653

654 Ofir Nachum, Yinlam Chow, Bo Dai, and Lihong Li. Dualdice: Behavior-agnostic estimation of  
 655 discounted stationary distribution corrections. *Advances in neural information processing systems*,  
 656 32, 2019.

657

658 Reiichiro Nakano, Jacob Hilton, Suchir Balaji, Jeff Wu, Long Ouyang, Christina Kim, Christopher  
 659 Hesse, Shantanu Jain, Vineet Kosaraju, William Saunders, et al. Webgpt: Browser-assisted  
 660 question-answering with human feedback. *arXiv preprint arXiv:2112.09332*, 2021.

661

662 Ian Osband and Benjamin Van Roy. Near-optimal reinforcement learning in factored mdps. *Advances  
 in Neural Information Processing Systems*, 27, 2014.

663

664 Long Ouyang, Jeffrey Wu, Xu Jiang, Diogo Almeida, Carroll Wainwright, Pamela Mishkin, Chong  
 665 Zhang, Sandhini Agarwal, Katarina Slama, Alex Ray, et al. Training language models to follow  
 666 instructions with human feedback. *Advances in neural information processing systems*, 35:27730–  
 667 27744, 2022.

668

669 Aldo Pacchiano, Aadirupa Saha, and Jonathan Lee. Dueling rl: reinforcement learning with trajectory  
 670 preferences. *arXiv preprint arXiv:2111.04850*, 2021.

671

672 Alizée Pace, Bernhard Schölkopf, Gunnar Rätsch, and Giorgia Ramponi. Preference elicitation for  
 673 offline reinforcement learning. *arXiv preprint arXiv:2406.18450*, 2024.

674

675 Jongjin Park, Younggyo Seo, Jinwoo Shin, Honglak Lee, Pieter Abbeel, and Kimin Lee. Surf:  
 676 Semi-supervised reward learning with data augmentation for feedback-efficient preference-based  
 677 reinforcement learning. *arXiv preprint arXiv:2203.10050*, 2022.

678

679 Rajkumar Ramamurthy, Prithviraj Ammanabrolu, Kianté Brantley, Jack Hessel, Rafet Sifa, Christian  
 680 Bauckhage, Hannaneh Hajishirzi, and Yejin Choi. Is reinforcement learning (not) for natural  
 681 language processing: Benchmarks, baselines, and building blocks for natural language policy  
 682 optimization. *arXiv preprint arXiv:2210.01241*, 2022.

683

684 Paria Rashidinejad, Banghua Zhu, Cong Ma, Jiantao Jiao, and Stuart Russell. Bridging offline rein-  
 685 forcement learning and imitation learning: A tale of pessimism. *Advances in Neural Information  
 686 Processing Systems*, 34:11702–11716, 2021.

687

688 Marc Rigter, Bruno Lacerda, and Nick Hawes. Rambo-rl: Robust adversarial model-based offline  
 689 reinforcement learning. *Advances in neural information processing systems*, 35:16082–16097,  
 2022.

690

691 Dorsa Sadigh, Anca Dragan, Shankar Sastry, and Sanjit Seshia. *Active preference-based learning of  
 692 reward functions*. 2017.

693

694 John Schulman, Philipp Moritz, Sergey Levine, Michael Jordan, and Pieter Abbeel. High-dimensional  
 695 continuous control using generalized advantage estimation. *arXiv preprint arXiv:1506.02438*,  
 696 2015.

697

698 Laixi Shi, Gen Li, Yuting Wei, Yuxin Chen, and Yuejie Chi. Pessimistic q-learning for offline  
 699 reinforcement learning: Towards optimal sample complexity. In *International conference on  
 700 machine learning*, pp. 19967–20025. PMLR, 2022.

701

702 Daniel Shin, Anca D Dragan, and Daniel S Brown. Benchmarks and algorithms for offline preference-  
 703 based reward learning. *arXiv preprint arXiv:2301.01392*, 2023.

704

705 Nisan Stiennon, Long Ouyang, Jeffrey Wu, Daniel Ziegler, Ryan Lowe, Chelsea Voss, Alec Radford,  
 706 Dario Amodei, and Paul F Christiano. Learning to summarize with human feedback. *Advances in  
 707 neural information processing systems*, 33:3008–3021, 2020.

702 Yihao Sun. Offlinerl-kit: An elegant pytorch offline reinforcement learning library. <https://github.com/yihaosun1124/OfflineRL-Kit>, 2023.

703

704

705 Yuval Tassa, Tom Erez, and Emanuel Todorov. Synthesis and stabilization of complex behaviors  
706 through online trajectory optimization. In *2012 IEEE/RSJ International Conference on Intelligent  
707 Robots and Systems*, pp. 4906–4913. IEEE, 2012.

708

709 Masatoshi Uehara and Wen Sun. Pessimistic model-based offline RL: PAC bounds and posterior  
710 sampling under partial coverage. *CoRR*, abs/2107.06226, 2021a. URL <https://arxiv.org/abs/2107.06226>.

711

712 Masatoshi Uehara and Wen Sun. Pessimistic model-based offline reinforcement learning under partial  
713 coverage. *arXiv preprint arXiv:2107.06226*, 2021b.

714

715 Martin J Wainwright. *High-dimensional statistics: A non-asymptotic viewpoint*, volume 48. Cam-  
716 bridge university press, 2019.

717

718 Garrett Warnell, Nicholas Waytowich, Vernon Lawhern, and Peter Stone. Deep tamer: Interactive  
719 agent shaping in high-dimensional state spaces. *Proceedings of the AAAI Conference on Artificial  
Intelligence*, 32(1), Apr. 2018. doi: 10.1609/aaai.v32i1.11485. URL <https://ojs.aaai.org/index.php/AAAI/article/view/11485>.

720

721 Christian Wirth, Riad Akrou, Gerhard Neumann, and Johannes Fürnkranz. A survey of preference-  
722 based reinforcement learning methods. *Journal of Machine Learning Research*, 18(136):1–46,  
723 2017. URL <http://jmlr.org/papers/v18/16-634.html>.

724

725 Jeff Wu, Long Ouyang, Daniel M Ziegler, Nisan Stiennon, Ryan Lowe, Jan Leike, and Paul Christiano.  
726 Recursively summarizing books with human feedback. *arXiv preprint arXiv:2109.10862*, 2021.

727

728 Tengyang Xie, Ching-An Cheng, Nan Jiang, Paul Mineiro, and Alekh Agarwal. Bellman-consistent  
729 pessimism for offline reinforcement learning. *Advances in neural information processing systems*,  
34:6683–6694, 2021.

730

731 Tianhe Yu, Deirdre Quillen, Zhanpeng He, Ryan Julian, Karol Hausman, Chelsea Finn, and Sergey  
732 Levine. Meta-world: A benchmark and evaluation for multi-task and meta reinforcement learning.  
733 In *Conference on robot learning*, pp. 1094–1100. PMLR, 2020a.

734

735 Tianhe Yu, Garrett Thomas, Lantao Yu, Stefano Ermon, James Y Zou, Sergey Levine, Chelsea Finn,  
736 and Tengyu Ma. Mopo: Model-based offline policy optimization. *Advances in Neural Information  
Processing Systems*, 33:14129–14142, 2020b.

737

738 Tianhe Yu, Aviral Kumar, Rafael Rafailov, Aravind Rajeswaran, Sergey Levine, and Chelsea Finn.  
739 Combo: Conservative offline model-based policy optimization. *Advances in neural information  
processing systems*, 34:28954–28967, 2021.

740

741 Wenhao Zhan, Baihe Huang, Audrey Huang, Nan Jiang, and Jason Lee. Offline reinforcement  
742 learning with realizability and single-policy concentrability. In *Conference on Learning Theory*,  
743 pp. 2730–2775. PMLR, 2022.

744

745 Wenhao Zhan, Masatoshi Uehara, Nathan Kallus, Jason D Lee, and Wen Sun. Provable offline  
746 preference-based reinforcement learning. *arXiv preprint arXiv:2305.14816*, 2023a.

747

748 Wenhao Zhan, Masatoshi Uehara, Wen Sun, and Jason D. Lee. How to query human feedback  
749 efficiently in RL? In *ICML 2023 Workshop The Many Facets of Preference-Based Learning*, 2023b.  
URL <https://openreview.net/forum?id=2ZaszaehLs>.

750

751 Banghua Zhu, Michael Jordan, and Jiantao Jiao. Principled reinforcement learning with human  
752 feedback from pairwise or k-wise comparisons. In *International Conference on Machine Learning*,  
753 pp. 43037–43067. PMLR, 2023.

754

755 Daniel M Ziegler, Nisan Stiennon, Jeffrey Wu, Tom B Brown, Alec Radford, Dario Amodei, Paul  
Christiano, and Geoffrey Irving. Fine-tuning language models from human preferences. *arXiv  
preprint arXiv:1909.08593*, 2019.

# Appendix

## Table of Contents

A	Additional Related Work	15
B	Technical Proofs for General Function Approximation	16
C	Optimization Error	22
D	Technical Proofs for KNRs	25
E	Technical Proofs for Factored Models	29
F	Experimental Setup	32
G	Implementation Details	33
H	Visualization of Training Dynamics	36
J	Additional Experimental Results	36

## A RELATED WORK

**Offline Preference-based Reinforcement Learning.** Recent advancements in offline PbRL have investigated a variety of methods for incorporating preference feedback into policy learning. Some of these approaches rely on explicit reward modeling, while others aim to bypass it altogether. For instance, OPRL [Shin et al., 2023] introduces an active querying mechanism over offline data to infer a reward model from preferences, which is subsequently used in standard offline RL pipelines. PT [Kim et al., 2023] proposes a transformer-based reward model designed to capture non-Markovian dependencies in human feedback. In contrast, IPL [Hejna & Sadigh, 2023] avoids reward modeling entirely by directly optimizing a Q-function aligned with preferences through the inverse Bellman operator. Similarly, DPPO [An et al., 2023] formulates preference learning as a contrastive objective, enabling direct policy optimization based on preference data without estimating an intermediate reward function. While these methods demonstrate promising empirical performance, they generally lack sample complexity guarantees, which raises concerns about their theoretical robustness.

To overcome these limitations, recent works have proposed offline PbRL algorithms with theoretical guarantees under partial data coverage. For instance, [Zhu et al., 2023] provides the first sample complexity results under linear reward models, while subsequent works [Zhan et al., 2023a; Pace et al., 2024] extend these to general function approximation using confidence-set-based policy optimization. Yet, constructing and optimizing over such sets is often computationally intensive. In the recent work [Kang & Oh, 2025], their algorithms either assume known transition dynamics or require fitting an extra value function that depends on the learned transition model via Bellman recursion to perform conservatism. This allows the value function to locally smooth over gaps in data coverage—if the value function is well-approximated. However, this smoothing-based mitigation strategy intrinsically requires the realizability condition on the value function and does not guarantee near-optimal regret under partial coverage.

In contrast, our work proposes a model-based offline PbRL framework that encodes conservatism implicitly via relative performance objectives, avoiding confidence set construction and value function estimation. By learning both the reward and transition models from offline data and using them for conservative planning, our approach achieves PAC guarantees under general function approximation, without assuming known dynamics. Moreover, when applied to structured settings (e.g., kernelized nonlinear regulators or factored models), it yields refined generalization guarantees.

**Preference-based Reinforcement Learning.** Unlike traditional RL, which relies on explicit numerical rewards for each state-action pair, preference-based RL infers a reward function by collecting pairwise preferences over trajectories [Wirth et al., 2017; Akroud et al., 2012]. Various strategies have been proposed for eliciting preferences, typically assuming access to either a known transition model or an environment that supports interaction or rollouts [Brown et al., 2020; Christiano et al., 2017; Chen et al., 2022; Pacchiano et al., 2021; Sadigh et al., 2017; Zhan et al., 2023b; Lindner et al., 2021; Stiennon et al., 2020; Park et al., 2022; Hejna III & Sadigh, 2023]. While effective in interactive or online settings, these assumptions limit the applicability of many PbRL methods in the offline setting, where the agent must learn solely from a fixed dataset without further interaction.

810    **Offline RL.** Offline RL has gained attention because it allows learning policies without interacting  
 811    with the environment, which is important in areas where safety concerns or data collection costs make  
 812    interaction difficult [Levine et al., 2020]. However, offline RL is also difficult because the available  
 813    data may not cover all relevant state-action pairs. This lack of coverage can cause errors during policy  
 814    learning. To address this issue, many algorithms have been proposed that introduce conservative  
 815    learning strategies to ensure reliable performance under limited data coverage [Zhan et al., 2022; Xie  
 816    et al., 2021; Liu et al., 2020; Jin et al., 2021; Kumar et al., 2020; Uehara & Sun, 2021b; Rashidinejad  
 817    et al., 2021; Shi et al., 2022; Li et al., 2024; Kidambi et al., 2020; Yu et al., 2021; Nachum et al.,  
 818    2019].

## 820    B TECHNICAL PROOFS FOR GENERAL FUNCTION APPROXIMATION

821    To begin with, we will introduce some technical notations used in this section to facilitate reading.

### 822    Summarization of Notations:

- 825    • We use  $\mathcal{R}$  to represent the function class for the reward model,  $\{\mathcal{P}_h\}_{h=0}^{H-1}$  to represent the  
 826    function class for transition dynamics. We use  $\mathcal{N}_{\mathcal{R}}(1/N)$  to represent the  $1/N$ -bracket  
 827    number for reward model function class  $\mathcal{R}$ , and  $\mathcal{N}_{\mathcal{P}}(1/N)$  to represent the  $1/N$ -bracket  
 828    number for transition dynamics function class  $\{\mathcal{P}_h\}_{h=0}^{H-1}$ .
- 829    • We use  $r^*$  to denote the ground-truth reward model,  $\{P_h^*\}_{h=0}^{H-1}$  to denote the ground-truth  
 830    transition dynamics at time steps  $h \in [0 : H - 1]$ . We use  $\hat{r}$  and  $\{\hat{P}_h\}_{h=0}^{H-1}$  to denote their  
 831    corresponding MLE estimators, respectively.
- 832    • Concentrability coefficient for reward:

$$834 \quad \mathfrak{C}_R(\pi) = \sup_{r \in \mathcal{R}} \frac{\mathbb{E}_{\tau^1 \sim d^\pi, \tau^0 \sim \mu_{ref}} [\|(r(\tau^1) - r(\tau^0)) - (r^*(\tau^1) - r^*(\tau^0))\|]}{\mathbb{E}_{\tau^1 \sim \mu, \tau^0 \sim \mu} [\|(r(\tau^1) - r(\tau^0)) - (r^*(\tau^1) - r^*(\tau^0))\|]}.$$

- 837    • Concentrability coefficient for transition:

$$838 \quad \mathfrak{C}_P(\pi) = \max_{h \in [0 : H - 1]} \sup_{P_h \in \mathcal{P}_h} \frac{\mathbb{E}_{(s,a) \sim d_h^\pi} [D_{TV}(P_h(\cdot|s,a), P_h^*(\cdot|s,a))] }{\mathbb{E}_{(s,a) \sim \mu_h} [D_{TV}(P_h(\cdot|s,a), P_h^*(\cdot|s,a))]}.$$

- 841    • Empirical regularizer for reward model:

$$843 \quad \mathcal{E}_1(r; \mathcal{D}) = \frac{1}{N} \sum_{n=1}^N \|(r(\tau^{n,1}) - r(\tau^{n,0})) - (\hat{r}(\tau^{n,1}) - \hat{r}(\tau^{n,0}))\|.$$

- 846    • Empirical regularizer for transition dynamics:

$$848 \quad \mathcal{E}_2(\{P_h\}_{h=0}^{H-1}; \mathcal{D}) = \frac{1}{N} \sum_{n=1}^N \sum_{h=0}^{H-1} \sum_{i=0}^1 \left\| P_h(s_{h+1}^{n,i} | s_h^{n,i}, a_h^{n,i}) - \hat{P}_h(s_{h+1}^{n,i} | s_h^{n,i}, a_h^{n,i}) \right\|.$$

851    **Lemma B.1.** Let  $M = (\{P_M^h\}_{h=0}^{H-1}, r_M)$ ,  $M' = (\{P_{M'}^h\}_{h=0}^{H-1}, r_{M'})$  be two MDPs defined over the  
 852    same state-action space and initial state. We define  $J_M(\pi) := J(\pi; r_M, \{P_M^h\}_{h=0}^{H-1})$ . For any policy  
 853     $\pi : \mathcal{S} \rightarrow \Delta(\mathcal{A}) \in \Pi$ . By Assumption 2, we have

$$855 \quad J_M(\pi) - J_{M'}(\pi) \\ 856 \quad \leq R_{\max} \sum_{h=0}^{H-1} \mathbb{E}_{s,a \sim d_{P_M^h}^\pi} [D_{TV}(P_M^h(\cdot|s,a), P_{M'}^h(\cdot|s,a))] + \mathbb{E}_{\tau \sim d_{\{P_M^h\}_{h=0}^{H-1}}^\pi} [r_M(\tau) - r_{M'}(\tau)].$$

860    **Proof of Lemma B.1.** To analyze the difference  $J_M(\pi) - J_{M'}(\pi)$ , we begin by expressing it as the  
 861    sum of two terms: one corresponding to the difference in rewards under the same dynamics, and  
 862    another capturing the difference induced by the change in transition dynamics. Specifically, we write

$$863 \quad J_M(\pi) - J_{M'}(\pi) = \mathbb{E}_{\tau \sim d_{\{P_M^h\}_{h=0}^{H-1}}^\pi} [r_M(\tau)] - \mathbb{E}_{\tau \sim d_{\{P_{M'}^h\}_{h=0}^{H-1}}^\pi} [r_{M'}(\tau)]$$

$$\begin{aligned}
&= \underbrace{\mathbb{E}_{\tau \sim d^{\pi}_{\{P_M^h\}_{h=0}^{H-1}}} [r_M(\tau) - r_{M'}(\tau)]}_{(A)} \\
&\quad + \underbrace{\left( \mathbb{E}_{\tau \sim d^{\pi}_{\{P_M^h\}_{h=0}^{H-1}}} [r_{M'}(\tau)] - \mathbb{E}_{\tau \sim d^{\pi}_{\{P_{M'}^h\}_{h=0}^{H-1}}} [r_{M'}(\tau)] \right)}_{(B)}.
\end{aligned}$$

Term (A) remains unchanged. Now we aim to bound term (B). By Lemma 9 in Uehara & Sun [2021a], we have

$$|(B)| \leq R_{\max} \sum_{h=0}^{H-1} \mathbb{E}_{s,a \sim d^{\pi}_{P_M^h}} [D_{TV}(P_M^h(\cdot|s,a), P_{M'}^h(\cdot|s,a))].$$

This completes the proof.  $\square$

**Lemma B.2.** *Zhan et al. [2023a]* For any reward model  $r \in \mathcal{R}$ , with probability at least  $1 - \delta$ , we have

$$\mathbb{E}_{\tau_0 \sim \mu, \tau_1 \sim \mu} [\|(r(\tau_1) - r(\tau_0)) - (r^*(\tau_1) - r^*(\tau_0))\|^2] \leq \frac{c\kappa^2 \log(\mathcal{N}_{\mathcal{R}}(1/N)/\delta)}{N},$$

where  $c > 0$  is a universal constant,  $\kappa := \frac{1}{\inf_{x \in [-r_{\max}, r_{\max}]} \Phi'(x)}$  measures the nonlinearity of the link function.

**Lemma B.3.** *Zhan et al. [2023a]* With probability at least  $1 - \delta$ , for all  $h \in [0 : H - 1]$ , it holds that

$$\begin{aligned}
&\mathbb{E}_{(s,a) \sim \mu_h} \left[ \left\| P_h^*(\cdot|s,a) - \hat{P}_h(\cdot|s,a) \right\|_{TV}^2 \right] \\
&\leq \frac{c \log(H\mathcal{N}_{\mathcal{P}}(1/N)/\delta)}{N},
\end{aligned}$$

where  $c > 0$  is a universal constant.

**Lemma B.4.** Let  $\{P_h^t\}_{h=0}^{H-1}$  be the transition models selected at line 5 of *Algorithm 1* corresponding to  $\pi_t$ , for iterations  $t \in [1 : T]$ . Then with probability at least  $1 - \delta$ , we have

$$\mathcal{E}_2(\{P_h^t\}_{h=0}^{H-1}; \mathcal{D}) \leq \frac{cHR_{\max}M_P}{\lambda_2} \sqrt{\frac{\log(H\mathcal{N}_{\mathcal{P}}(1/N)/\delta)}{N}} + \mathcal{E}_2(\{P_h^*\}_{h=0}^{H-1}; \mathcal{D}),$$

where  $c > 0$  is a universal constant.

**Proof of Lemma B.4.** Recall that in line 5 in *Algorithm 1*, the transition model  $\{P_h^t\}_{h=0}^{H-1}$  is selected as minimizers of

$$J(\pi_t; r, \{P_h\}_{h=0}^{H-1}) - \mathbb{E}_{\tau \sim \mu_{ref}} [r(\tau)] + \lambda_1 \mathcal{E}_1(r; \mathcal{D}) + \lambda_2 \mathcal{E}_2(\{P_h\}_{h=0}^{H-1}; \mathcal{D}),$$

where  $\pi_t$  is the policy at iteration  $t$ . So we have

$$\begin{aligned}
&J(\pi_t; r_t, \{P_h^t\}_{h=0}^{H-1}) - \mathbb{E}_{r \sim \mu_{ref}} [r_t(\tau)] + \lambda_1 \mathcal{E}_1(r_t; \mathcal{D}) + \lambda_2 \mathcal{E}_2(\{P_h^t\}_{h=0}^{H-1}; \mathcal{D}) \\
&= \min_{r \in \mathcal{R}, \{P_h \in \mathcal{P}_h\}_{h=0}^{H-1}} (J(\pi_t; r, \{P_h\}_{h=0}^{H-1}) - \mathbb{E}_{r \sim \mu_{ref}} [r(\tau)] + \lambda_1 \mathcal{E}_1(r; \mathcal{D}) + \lambda_2 \mathcal{E}_2(\{P_h\}_{h=0}^{H-1}; \mathcal{D})) \\
&\leq J(\pi_t; r_t, \{P_h^*\}_{h=0}^{H-1}) - \mathbb{E}_{r \sim \mu_{ref}} [r_t(\tau)] + \lambda_1 \mathcal{E}_1(r_t; \mathcal{D}) + \lambda_2 \mathcal{E}_2(\{P_h^*\}_{h=0}^{H-1}; \mathcal{D}).
\end{aligned}$$

Rearrange the equation above, and we have

$$\begin{aligned}
J(\pi_t; r_t, \{P_h^t\}_{h=0}^{H-1}) - J(\pi_t; r_t, \{P_h^*\}_{h=0}^{H-1}) &\leq \lambda_2 \mathcal{E}_2(\{P_h^*\}_{h=0}^{H-1}; \mathcal{D}) - \lambda_2 \mathcal{E}_2(\{P_h^t\}_{h=0}^{H-1}; \mathcal{D}) \\
&\leq \lambda_2 \mathcal{E}_2(\{P_h^*\}_{h=0}^{H-1}; \mathcal{D}).
\end{aligned} \tag{B.1}$$

918 We also have  
919

$$\begin{aligned}
& J(\pi_t; r_t, \{P_h^t\}_{h=0}^{H-1}) - \mathbb{E}_{r \sim \mu_{ref}}[r_t(\tau)] + \lambda_1 \mathcal{E}_1(r_t; \mathcal{D}) + \lambda_2 \mathcal{E}_2(\{P_h^t\}_{h=0}^{H-1}; \mathcal{D}) \\
&= \min_{r \in \mathcal{R}, P_h \in \mathcal{P}_h} (J(\pi_t; r, \{P_h\}_{h=0}^{H-1}) - \mathbb{E}_{r \sim \mu_{ref}}[r(\tau)] + \lambda_1 \mathcal{E}_1(r; \mathcal{D}) + \lambda_2 \mathcal{E}_2(\{P_h\}_{h=0}^{H-1}; \mathcal{D})) \\
&\leq J(\pi_t; r_t, \{\hat{P}_h\}_{h=0}^{H-1}) - \mathbb{E}_{r \sim \mu_{ref}}[r_t(\tau)] + \lambda_1 \mathcal{E}_1(r_t; \mathcal{D}) + \lambda_2 \mathcal{E}_2(\{\hat{P}_h\}_{h=0}^{H-1}; \mathcal{D}).
\end{aligned}$$

925 By rearranging the equation above, we can obtain  
926

$$\begin{aligned}
& \lambda_2 \mathcal{E}_2(\{P_h^t\}_{h=0}^{H-1}; \mathcal{D}) \\
&\leq \left| J(\pi_t; r_t, \{P_h^t\}_{h=0}^{H-1}) - J(\pi_t; r_t, \{\hat{P}_h\}_{h=0}^{H-1}) \right| \\
&= \left| J(\pi_t; r_t, \{P_h^t\}_{h=0}^{H-1}) - J(\pi_t; r_t, \{P_h^*\}_{h=0}^{H-1}) + J(\pi_t; r_t, \{P_h^*\}_{h=0}^{H-1}) - J(\pi_t; r_t, \{\hat{P}_h\}_{h=0}^{H-1}) \right| \\
&\leq \left| \lambda_2 \mathcal{E}_2(\{P_h^*\}_{h=0}^{H-1}; \mathcal{D}) + R_{\max} \sum_{h=0}^{H-1} \mathbb{E}_{s, a \sim d_h^{\pi_t}} [D_{TV}(\hat{P}_h(\cdot|s, a), P_h^*(\cdot|s, a))] \right| \\
&\leq \lambda_2 \mathcal{E}_2(\{P_h^*\}_{h=0}^{H-1}; \mathcal{D}) + H R_{\max} M_P \sqrt{\frac{c \log(H \mathcal{N}_P(1/N)/\delta)}{N}},
\end{aligned}$$

937 where  $M_P = \max_{t \in [1:T]} \max_{h \in [0:H-1]} \frac{\mathbb{E}_{(s, a) \sim d_h^{\pi_t}} [D_{TV}(P_h^t(\cdot|s, a), P_h^*(\cdot|s, a))] }{\mathbb{E}_{(s, a) \sim \mu_h} [D_{TV}(P_h^t(\cdot|s, a), P_h^*(\cdot|s, a))]}$ , the third step is by equation (B.1)  
938 and Lemma B.1. This completes the proof.  $\square$   
939

940 **Lemma B.5.** Let  $r^* \in \mathcal{R}$  denote the ground-truth reward model, and let  $\hat{r}$  denote the maximum  
941 likelihood estimator. Then with probability at least  $1 - \delta$ , we have  
942

$$\begin{aligned}
\mathcal{E}_1(r^*; \mathcal{D}) &= \frac{1}{N} \sum_{n=1}^N \| (r^*(\tau^{n,1}) - r^*(\tau^{n,0})) - (\hat{r}(\tau^{n,1}) - \hat{r}(\tau^{n,0})) \| \\
&\leq c \sqrt{\frac{\kappa^2 \log(\mathcal{N}_R(1/N)/\delta)}{N}} + c R_{\max} \sqrt{\frac{\log(\mathcal{N}_R(1/N)/\delta)}{N}},
\end{aligned}$$

943 where  $c > 0$  is a universal constant.  
944

945 **Proof of Lemma B.5.** By Assumption 2, both  $r^*$  and  $\hat{r}$  are bounded by  $R_{\max}$ , so for any pair of  
946 trajectories, we have  
947

$$\| (r^*(\tau^{(1)}) - r^*(\tau^{(0)})) - (\hat{r}(\tau^{(1)}) - \hat{r}(\tau^{(0)})) \| \leq 4R_{\max}.$$

948 Define  $f_r = (r^*(\tau^{(1)}) - r^*(\tau^{(0)})) - (\hat{r}(\tau^{(1)}) - \hat{r}(\tau^{(0)}))$ .  
949

950 By Hoeffding's inequality and union bound, we obtain  
951

$$\mathbb{P} \left( \left| \frac{1}{N} \sum_{n=1}^N \|f_r\| - \mathbb{E}[\|f_r\|] \right| \geq \epsilon \right) \leq 2\mathcal{N}_R(1/N) \exp \left( -\frac{2N\epsilon^2}{(4R_{\max})^2} \right).$$

952 Now solve for  $\epsilon$  such that the RHS  $\leq \delta$ , we get  
953

$$\epsilon = 4R_{\max} \sqrt{\frac{\log(2\mathcal{N}_R(1/N)/\delta)}{2N}}.$$

954 Meanwhile, from Lemma B.2, by Jensen's inequality, we also have  
955

$$\mathbb{E}[\|f_r\|^2] \leq \frac{ck^2 \log(\mathcal{N}_R(1/N)/\delta)}{N} \Rightarrow \mathbb{E}[\|f_r\|] \leq \sqrt{\frac{ck^2 \log(\mathcal{N}_R(1/N)/\delta)}{N}}.$$

972 Putting everything together, we obtain  
 973

$$974 \quad \mathcal{E}_1(r^*; \mathcal{D}) \leq c \sqrt{\frac{\kappa^2 \log(\mathcal{N}_{\mathcal{R}}(1/N)/\delta)}{N}} + cR_{\max} \sqrt{\frac{\log(\mathcal{N}_{\mathcal{R}}(1/N)/\delta)}{N}},$$

975 where  $c > 0$  is a universal constant. This completes the proof.  $\square$   
 976

977  
 978  
 979  
**Lemma B.6.** Let  $\{P_h^*\}_{h=0}^{H-1}$  denote the ground-truth transition dynamics at time steps  $h \in [0 : H-1]$   
 980 and let  $\{\hat{P}_h\}_{h=0}^{H-1}$  denote the maximum likelihood estimator. Then, with probability at least  $1 - \delta$ , we  
 981 have  
 982

$$983 \quad \mathcal{E}_2(\{P_h^*\}_{h=0}^{H-1}; \mathcal{D}) = \frac{1}{N} \sum_{n=1}^N \sum_{h=0}^{H-1} \sum_{i=0}^1 \left\| P_h^*(s_{h+1}^{n,i} | s_h^{n,i}, a_h^{n,i}) - \hat{P}_h(s_{h+1}^{n,i} | s_h^{n,i}, a_h^{n,i}) \right\|$$

$$984 \quad \leq cH \sqrt{\frac{\log(H\mathcal{N}_{\mathcal{P}}(1/N)/\delta)}{N}},$$

985 where  $c > 0$  is a universal constant.  
 986

987  
 988  
**Proof of Lemma B.6.** Since the  $N$  trajectory pairs are sampled i.i.d, we first take expectation over  
 989 the data distribution  $\mu_h$ , and average over  $n$   
 990

$$991 \quad \mathbb{E}[\mathcal{E}_2(\{P_h^*\}_{h=0}^{H-1}; \mathcal{D})] = \sum_{h=0}^{H-1} \sum_{i=0}^1 \mathbb{E}_{(s_h, a_h) \sim \mu_{i,h}} \left[ \left\| P_h^*(\cdot | s_h, a_h) - \hat{P}_h(\cdot | s_h, a_h) \right\| \right].$$

992 By Lemma B.3 and Jensen's inequality, summing over all  $h$  and  $i$  we obtain  
 993

$$994 \quad \mathbb{E}[\mathcal{E}_2(\{P_h^*\}_{h=0}^{H-1}; \mathcal{D})] \leq cH \sqrt{\frac{\log(H\mathcal{N}_{\mathcal{P}}(1/N)/\delta)}{N}},$$

995  
 996 where  $c > 0$  is a universal constant. Applying Hoeffding's inequality and union bound over the  
 997 transition dynamics function class  
 998

$$1000 \quad P \left( \left| \frac{1}{N} \sum_{n=1}^N \mathcal{E}_2(\{P_h^*\}_{h=0}^{H-1}; \mathcal{D}) - \mathbb{E}[\mathcal{E}_2(\{P_h^*\}_{h=0}^{H-1}; \mathcal{D})] \right| \geq \epsilon \right) \leq 2H\mathcal{N}_{\mathcal{P}}(1/N) \exp \left( -\frac{N\epsilon^2}{2H^2} \right).$$

1001  
 1002 Solve for  $\epsilon$  such that the RHS is bounded by  $\delta$ , we obtain  
 1003

$$1004 \quad \epsilon = H \sqrt{\frac{2 \log(2H\mathcal{N}_{\mathcal{P}}(1/N)/\delta)}{N}}.$$

1005  
 1006 By applying Lemma B.4, we have  
 1007

$$1008 \quad \mathcal{E}_2(\{P_h^t\}_{h=0}^{H-1}; \mathcal{D})$$

$$1009 \quad \leq \frac{cHR_{\max}M_P}{\lambda_2} \sqrt{\frac{\log(H\mathcal{N}_{\mathcal{P}}(1/N)/\delta)}{N}} + cH \sqrt{\frac{\log(H\mathcal{N}_{\mathcal{P}}(1/N)/\delta)}{N}}.$$

1010 This completes the proof.  $\square$   
 1011

1012  
 1013  
**Lemma B.7.** Let  $\pi_t$  denote the policy at iterations  $t \in [1 : T]$ . For the associated reward function  $r_t$ ,  
 1014 transition dynamics  $\{P_h^t\}_{h=0}^{H-1}$  selected in line 5 of the [Algorithm 1](#), we have  
 1015

$$1016 \quad J(\pi_t) \geq J\left(\pi_t; r_t, \{P_h^t\}_{h=0}^{H-1}\right) - \mathbb{E}_{\tau \sim \mu_{ref}}[r_t(\tau)] + \mathbb{E}_{\tau \sim \mu_{ref}}[r^*(\tau)]$$

$$1017 \quad - \lambda_1 \mathcal{E}_1(r^*; \mathcal{D}) - \lambda_2 \mathcal{E}_2(\{P_h^t\}_{h=0}^{H-1}; \mathcal{D}).$$

1026 **Proof of Lemma B.7.** Please recall that  $J(\pi_t) = J(\pi_t; r^*, \{P_h^*\}_{h=0}^{H-1})$ . So we have  
1027

$$\begin{aligned}
1028 \quad J(\pi_t) &= J(\pi_t) - \mathbb{E}_{\tau \sim \mu_{ref}}[r^*(\tau)] + \lambda_1 \mathcal{E}_1(r^*; \mathcal{D}) + \lambda_2 \mathcal{E}_2(\{P_h^*\}_{h=0}^{H-1}; \mathcal{D}) + \mathbb{E}_{\tau \sim \mu_{ref}}[r^*(\tau)] \\
1029 &\quad - \lambda_1 \mathcal{E}_1(r^*; \mathcal{D}) - \lambda_2 \mathcal{E}_2(\{P_h^*\}_{h=0}^{H-1}; \mathcal{D}) \\
1030 &\geq \min_{r, \{P_h\}_{h=0}^{H-1}} (J(\pi_t; r, \{P_h\}_{h=0}^{H-1}) - \mathbb{E}_{\tau \sim \mu_{ref}}[r(\tau)] + \lambda_1 \mathcal{E}_1(r; \mathcal{D}) \\
1031 &\quad + \lambda_2 \mathcal{E}_2(\{P_h\}_{h=0}^{H-1}; \mathcal{D})) + \mathbb{E}_{\tau \sim \mu_{ref}}[r^*(\tau)] - \lambda_1 \mathcal{E}_1(r^*; \mathcal{D}) - \lambda_2 \mathcal{E}_2(\{P_h^*\}_{h=0}^{H-1}; \mathcal{D}) \\
1032 &= J(\pi_t; r_t, \{P_h^t\}_{h=0}^{H-1}) - \mathbb{E}_{\tau \sim \mu_{ref}}[r_t(\tau)] + \lambda_1 \mathcal{E}_1(r_t; \mathcal{D}) + \lambda_2 \mathcal{E}_2(\{P_h^t\}_{h=0}^{H-1}; \mathcal{D}) \\
1033 &\quad + \mathbb{E}_{\tau \sim \mu_{ref}}[r^*(\tau)] - \lambda_1 \mathcal{E}_1(r^*; \mathcal{D}) - \lambda_2 \mathcal{E}_2(\{P_h^*\}_{h=0}^{H-1}; \mathcal{D}) \\
1034 &\geq J(\pi_t; r_t, \{P_h^t\}_{h=0}^{H-1}) - \mathbb{E}_{\tau \sim \mu_{ref}}[r_t(\tau)] + \mathbb{E}_{\tau \sim \mu_{ref}}[r^*(\tau)] \\
1035 &\quad - \lambda_1 \mathcal{E}_1(r^*; \mathcal{D}) - \lambda_2 \mathcal{E}_2(\{P_h^*\}_{h=0}^{H-1}; \mathcal{D}),
\end{aligned}$$

1041 where the third step is by the optimality of the  $r_t$  and  $\{P_h^t\}_{h=0}^{H-1}$ . This completes the proof.  $\square$   
1042

1043 Now we want to make some modifications to the Lemma B.1 to serve for proof of the main theorem  
1044 later.

1045  
1046 **Lemma B.8.** Let  $\pi \in \Pi$  be an arbitrary policy. Then, for the reward model  $r_t$  selected in Line 5 of  
1047 *Algorithm 1* corresponding to  $\pi_t$ , with probability at least  $1 - \delta$ , for all  $t \in [1 : T]$ , we have  
1048

$$1049 \quad \mathbb{E}_{\tau^1 \sim d^\pi, \tau^0 \sim \mu_{ref}}[\|r_t(\tau^1) - r_t(\tau^0) - (r^*(\tau^1) - r^*(\tau^0))\|] \leq c \mathfrak{C}_R(\pi) \sqrt{\frac{\kappa^2 \log(\mathcal{N}_R(1/N)/\delta)}{N}},$$

1050 where  $c > 0$  is a universal constant.

1051  
1052 **Proof of Lemma B.8.**

$$\begin{aligned}
1053 \quad &\mathbb{E}_{\tau^1 \sim d^\pi, \tau^0 \sim \mu_{ref}}[\|r_t(\tau^1) - r_t(\tau^0) - (r^*(\tau^1) - r^*(\tau^0))\|] \\
1054 &\leq \mathfrak{C}_R(\pi) \mathbb{E}_{\tau^1 \sim \mu, \tau^0 \sim \mu}[\|r_t(\tau^1) - r_t(\tau^0) - (r^*(\tau^1) - r^*(\tau^0))\|] \\
1055 &\leq c \mathfrak{C}_R(\pi) \sqrt{\frac{\kappa^2 \log(\mathcal{N}_R(1/N)/\delta)}{N}},
\end{aligned}$$

1056 where the second step is by Lemma B.2. This completes the proof.  $\square$   
1057

1058 **Lemma B.9.** Let  $\pi \in \Pi$  be an arbitrary policy. Then, for the transition model  $\{P_h^t\}_{h=0}^{H-1}$  selected in  
1059 Line 5 of *Algorithm 1* corresponding to  $\pi_t$ , with probability at least  $1 - \delta$ , for all  $t \in [1 : T]$ , we have  
1060

$$\begin{aligned}
1061 \quad &\sum_{h=0}^{H-1} \mathbb{E}_{d_h^\pi} [D_{TV}(P_h^t(\cdot|s, a), P_h^*(\cdot|s, a))] \\
1062 &\leq c \mathfrak{C}_P(\pi) H \left( \frac{R_{\max} M_P}{\lambda_2} \sqrt{\frac{\log(HN_P(1/N)/\delta)}{N}} + \sqrt{\frac{\log(HN_P(1/N)/\delta)}{N}} \right),
\end{aligned}$$

1063 where  $c > 0$  is a universal constant.

1064  
1065 **Proof of Lemma B.9.**

$$\begin{aligned}
1066 \quad &\sum_{h=0}^{H-1} \mathbb{E}_{d_h^\pi} [D_{TV}(P_h^t(\cdot|s, a), P_h^*(\cdot|s, a))] \\
1067 &\leq \mathfrak{C}_P(\pi) \sum_{h=0}^{H-1} \mathbb{E}_{\mu_h} [D_{TV}(P_h^t(\cdot|s, a), P_h^*(\cdot|s, a))]
\end{aligned}$$

$$\begin{aligned}
& \leq \mathfrak{C}_P(\pi) \sum_{h=0}^{H-1} \left( \underbrace{\mathbb{E}_{\mu_h} \left[ \left\| P_h^t(\cdot|s, a), \widehat{P}_h(\cdot|s, a) \right\|_{TV} \right]}_{(a)} + \underbrace{\mathbb{E}_{\mu_h} \left[ \left\| P_h^*(\cdot|s, a), \widehat{P}_h(\cdot|s, a) \right\|_{TV} \right]}_{(b)} \right).
\end{aligned}$$

The bound for term (b) can be obtained from Lemma B.3. Now we want to bound term (a) by Hoeffding's inequality and apply the union bound

$$\begin{aligned}
& \mathbb{P} \left( \left| \frac{1}{N} \sum_{n=1}^N \mathcal{E}_2(\{P_h^t\}_{h=0}^{H-1}; \mathcal{D}) - \sum_{h=0}^{H-1} \mathbb{E}_{\mu_h} \left[ \left\| P_h^t(\cdot|s, a), \widehat{P}_h(\cdot|s, a) \right\|_{TV} \right] \right| \geq \epsilon \right) \\
& \leq 2H\mathcal{N}_P(1/N) \exp \left( -\frac{N\epsilon^2}{2H^2} \right),
\end{aligned}$$

where the bound for  $\mathcal{E}_2(\{P_h^t\}_{h=0}^{H-1})$  can be obtained from Lemma B.6. Solving for  $\epsilon$  such that the RHS is at most  $\delta$

$$\epsilon = H \sqrt{\frac{2 \log(2H\mathcal{N}_P(1/N)/\delta)}{N}}.$$

Combining all the equations above completes the proof.  $\square$

We are now ready to establish the proof of the main theorem. Before we start, we define  $J_{\mathcal{M}_t}(\pi) := J(\pi, r_t, \{P_h^t\}_{h=0}^{H-1})$ , where  $r_t$  and  $\{P_h^t\}_{h=0}^{H-1}$  are conservatively estimated models corresponding to  $\pi_t$  and please recall that  $J(\pi) = J(\pi; r^*, \{P_h^*\}_{h=0}^{H-1})$ .

### Proof of Theorem 4.1.

$$\begin{aligned}
& J(\pi) - J(\pi^{\text{ALG}}) \\
& = \frac{1}{T} \sum_{t=1}^T (J(\pi) - J(\pi_t)) \\
& \leq \frac{1}{T} \sum_{t=1}^T (J(\pi) - (\mathbb{E}_{\tau \sim \mu_{ref}}[r^*(\tau)] - \mathbb{E}_{\tau \sim \mu_{ref}}[r_t(\tau)]) - J_{\mathcal{M}_t}(\pi_t)) \\
& \quad + \lambda_1 \mathcal{E}_1(r^*; \mathcal{D}) + \lambda_2 \mathcal{E}_2(\{P_h^*\}_{h=0}^{H-1}; \mathcal{D}) \\
& \leq \frac{1}{T} \sum_{t=1}^T (J_{\mathcal{M}_t}(\pi) + R_{\max} \sum_{h=0}^{H-1} \mathbb{E}_{(s,a) \sim d_h^\pi} [D_{TV}(P_h^t(\cdot|s, a), P_h^*(\cdot|s, a))] \\
& \quad + \mathbb{E}_{\tau \sim d^\pi} [r^*(\tau) - r_t(\tau)] - (\mathbb{E}_{\tau \sim \mu_{ref}}[r^*(\tau)] - \mathbb{E}_{\tau \sim \mu_{ref}}[r_t(\tau)]) - J_{\mathcal{M}_t}(\pi_t)) \\
& \quad + \lambda_1 \mathcal{E}_1(r^*; \mathcal{D}) + \lambda_2 \mathcal{E}_2(\{P_h^*\}_{h=0}^{H-1}; \mathcal{D}) \\
& \leq \frac{1}{T} \sum_{t=1}^T (J_{\mathcal{M}_t}(\pi) + R_{\max} \sum_{h=0}^{H-1} \mathbb{E}_{(s,a) \sim d_h^\pi} [D_{TV}(P_h^t(\cdot|s, a), P_h^*(\cdot|s, a))] \\
& \quad + \mathbb{E}_{\tau^1 \sim d^\pi, \tau^0 \sim \mu_{ref}} [\|r^*(\tau^1) - r_t(\tau^1) - (r^*(\tau^0) - r_t(\tau^0))\|] - J_{\mathcal{M}_t}(\pi_t)) \\
& \quad + \lambda_1 \mathcal{E}_1(r^*; \mathcal{D}) + \lambda_2 \mathcal{E}_2(\{P_h^*\}_{h=0}^{H-1}; \mathcal{D}) \\
& \lesssim \frac{1}{T} \sum_{t=1}^T (J_{\mathcal{M}_t}(\pi) - J_{\mathcal{M}_t}(\pi_t)) + \lambda_1 \mathcal{E}_1(r^*; \mathcal{D}) + \lambda_2 \mathcal{E}_2(\{P_h^*\}_{h=0}^{H-1}; \mathcal{D}) \\
& \quad + H R_{\max} \mathfrak{C}_P(\pi) \left( \frac{R_{\max} M_P}{\lambda_2} \sqrt{\frac{\log(HN_P(1/N)/\delta)}{N}} + \sqrt{\frac{\log(HN_P(1/N)/\delta)}{N}} \right) \\
& \quad + \mathfrak{C}_R(\pi) \sqrt{\frac{\kappa^2 \log(\mathcal{N}_R(1/N)/\delta)}{N}} \\
& \lesssim R_{\max} \sqrt{\frac{\log |\mathcal{A}|}{T}} + \lambda_1 \mathcal{E}_1(r^*; \mathcal{D}) + \lambda_2 \mathcal{E}_2(\{P_h^*\}_{h=0}^{H-1}; \mathcal{D})
\end{aligned}$$

$$\begin{aligned}
& + H R_{\max} \mathfrak{C}_P(\pi) \left( \frac{R_{\max} M_P}{\lambda_2} \sqrt{\frac{\log(HN_P(1/N)/\delta)}{N}} + \sqrt{\frac{\log(2HN_P(1/N)/\delta)}{N}} \right) \\
& + \mathfrak{C}_R(\pi) \sqrt{\frac{\kappa^2 \log(\mathcal{N}_R(1/N)/\delta)}{N}} \\
& \lesssim R_{\max} \sqrt{\frac{\log |\mathcal{A}|}{T}} + \lambda_1 \left( \sqrt{\frac{\kappa^2 \log(\mathcal{N}_R(1/N)/\delta)}{N}} + 4R_{\max} \sqrt{\frac{\log(2\mathcal{N}_R(1/N)/\delta)}{2N}} \right) \\
& + \lambda_2 \left( H \sqrt{\frac{\log(HN_P(1/N)/\delta)}{N}} + H \sqrt{\frac{2\log(2HN_P(1/N)/\delta)}{N}} \right) \\
& + H R_{\max} \mathfrak{C}_P(\pi) \left( \frac{R_{\max} M_P}{\lambda_2} \sqrt{\frac{\log(HN_P(1/N)/\delta)}{N}} + \sqrt{\frac{\log(2HN_P(1/N)/\delta)}{N}} \right) \\
& + \mathfrak{C}_R(\pi) \sqrt{\frac{\kappa^2 \log(\mathcal{N}_R(1/N)/\delta)}{N}},
\end{aligned}$$

where the second step is by Lemma B.7, the third step is by Lemma B.1, the fifth step is by Lemma B.9, Lemma B.8. the sixth step is by Lemma C.4, the seventh step is by Lemma B.5, Lemma B.6. Substituting  $\lambda_1 = \mathcal{O}(\mathfrak{C}_R(\pi))$ ,  $\lambda_2 = \mathcal{O}(R_{\max} \sqrt{\mathfrak{C}_P(\pi) M_P})$  completes the proof.  $\square$

## C OPTIMIZATION ERROR

For simplicity, we assume that the transition model  $P_h^t$  is homogeneous across all steps  $h \in [0 : H-1]$ . That is, we write  $P_t := P_h^t$  for all  $h$ . This simplification is made only for notational clarity and does not affect the correctness of the result.

For each iteration  $t \in [1 : T]$ , the algorithm proceeds as follows:

### Step 1. Model Selection:

Let the reward model  $\hat{r}_t$  and transition models  $P_t$  be selected by solving the following penalized objective

$$r_t, P_t = \min_{r, P} J(\pi_t; r, P) - \mathbb{E}_{\tau \sim \mu_{ref}}[r(\tau)] + \lambda_1 \mathcal{E}_1(r; \mathcal{D}) + \lambda_2 \mathcal{E}_2(P; \mathcal{D}).$$

### Step 2. Policy Improvement:

Update the policy using an exponentiated update rule based on the estimated reward signal

$$\pi_{t+1}(a|s) \propto \pi_t(a|s) \exp \left( \eta \mathbb{E}_{d_{P_t}^{\pi_t}}[r_t(\tau)|s, a] \right).$$

Let  $J_{\mathcal{M}_t}(\pi)$  denote the expected return under reward model  $r_t$  and transition dynamics  $P_t$ . We define the cumulative regret over  $T$  iterations as

$$\mathfrak{R}_T := \max_{\pi \in \Pi} \sum_{t=1}^T (J_{\mathcal{M}_t}(\pi) - J_{\mathcal{M}_t}(\pi_t)).$$

Additionally, define the entropy-like regularization function

$$\psi_s(\pi) := \frac{1}{\eta} \sum_{a \in \mathcal{A}} \pi(a|s) \log \pi(a|s).$$

**Lemma C.1.** *Let  $\pi : \mathcal{S} \rightarrow \Delta(\mathcal{A}) \in \Pi$  be an arbitrary policy. Then for any state  $s \in \mathcal{S}$ , the following inequality holds*

$$\sum_{t=1}^T \left\langle \pi_{t+1}(\cdot|s), \mathbb{E}_{d_{P_t}^{\pi_t}}[\hat{r}_t(\tau)|s, \cdot] \right\rangle - \psi_s(\pi_1) \geq \sum_{t=1}^T \left\langle \pi(\cdot|s), \mathbb{E}_{d_{P_t}^{\pi_t}}[\hat{r}_t(\tau)|s, \cdot] \right\rangle - \psi_s(\pi).$$

1188 **Proof of Lemma C.1.** We prove the results via mathematical induction over  $T$  by following [Xie  
1189 et al., 2021]. When  $T = 0$ , both sides of the inequality are zero. This holds because no iterations are  
1190 executed, and we define  $\psi_s(\pi_1)$  to be the entropy of the initial uniform policy. Thus, the inequality  
1191 trivially holds.

1192 Assume the statement holds for  $T = T'$ . That is,

$$1194 \sum_{t=1}^{T'} \left\langle \pi_{t+1}(\cdot|s), \mathbb{E}_{d_{P_t}^{\pi_t}} [\hat{r}_t(\tau)|s, \cdot] \right\rangle - \psi_s(\pi_1) \geq \sum_{t=1}^{T'} \left\langle \pi(\cdot|s), \mathbb{E}_{d_{P_t}^{\pi_t}} [\hat{r}_t(\tau)|s, \cdot] \right\rangle - \psi_s(\pi).$$

1197 We want to prove it for  $T = T' + 1$ . Consider:  $\sum_{t=1}^{T'+1} \left\langle \pi_{t+1}(\cdot|s), \mathbb{E}_{d_{P_t}^{\pi_t}} [\hat{r}_t(\tau)|s, \cdot] \right\rangle - \psi_s(\pi_1)$ .

1200 We can decompose this as

$$\begin{aligned} 1201 & \sum_{t=1}^{T'+1} \left\langle \pi_{t+1}(\cdot|s), \mathbb{E}_{d_{P_t}^{\pi_t}} [\hat{r}_t(\tau)|s, \cdot] \right\rangle - \psi_s(\pi_1) \\ 1202 &= \sum_{t=1}^{T'} \left\langle \pi_{t+1}(\cdot|s), \mathbb{E}_{d_{P_t}^{\pi_t}} [\hat{r}_t(\tau)|s, \cdot] \right\rangle - \psi_s(\pi_1) + \left\langle \pi_{T'+2}(\cdot|s), \mathbb{E}_{d_{P_{T+1}}^{\pi_{T+1}}} [\hat{r}_{T'+1}(\tau)|s, \cdot] \right\rangle \\ 1203 &\geq \sum_{t=1}^{T'} \langle \pi, \mathbb{E}_{d_{P_t}^{\pi_t}} [\hat{r}_t(\tau)|s, \cdot] \rangle - \psi_s(\pi_{T'+2}) + \left\langle \pi_{T'+2}(\cdot|s, \cdot), \mathbb{E}_{d_{P_{T+1}}^{\pi_{T+1}}} [\hat{r}_{T'+1}(\tau)|s, \cdot] \right\rangle \\ 1204 &= \sum_{t=1}^{T'+1} \langle \pi, \mathbb{E}_{d_{P_t}^{\pi_t}} [\hat{r}_t(\tau)|s, \cdot] \rangle - \psi_s(\pi_{T'+2}) \\ 1205 &\geq \sum_{t=1}^{T'+1} \langle \pi, \mathbb{E}_{d_{P_t}^{\pi_t}} [\hat{r}_t(\tau)|s, \cdot] \rangle - \psi_s(\pi), \end{aligned}$$

1216 where the second step is by the induction hypothesis, the fourth step is by the optimality of  $\pi_{T'+2}(\cdot|s)$ ,  
1217 i.e.,  $\pi_{T'+2} = \arg \max_{\pi'} \left\{ \left\langle \pi'(\cdot|s), \mathbb{E}_{d_{P_{T+1}}^{\pi_{T+1}}} [\hat{r}_{T'+1}(\tau)|s, \cdot] \right\rangle - \psi_s(\pi') \right\}$ . The proof is completed.

1218  $\square$

1221 **Lemma C.2.** Let  $\pi \in \Pi$  be an arbitrary policy. For any state  $s \in \mathcal{S}$ , The following inequality holds

$$1224 \sum_{t=1}^T \langle \pi(\cdot|s) - \pi_t(\cdot|s), \mathbb{E}_{d_{P_t}^{\pi_t}} [r_t(\tau)|s, \cdot] \rangle \leq \sum_{t=1}^T \langle \pi_{t+1}(\cdot|s) - \pi_t(\cdot|s), \mathbb{E}_{d_{P_t}^{\pi_t}} [r_t(\tau)|s, \cdot] \rangle - \psi_s(\pi_1).$$

1228 **Proof of Lemma C.2.** We begin by writing the LHS as

$$\begin{aligned} 1230 & \sum_{t=1}^T \left\langle \pi(\cdot|s) - \pi_t(\cdot|s), \mathbb{E}_{d_{P_t}^{\pi_t}} [r_t(\tau)|s, \cdot] \right\rangle \\ 1231 &= \sum_{t=1}^T \left( \left\langle \pi(\cdot|s), \mathbb{E}_{d_{P_t}^{\pi_t}} [r_t(\tau)|s, \cdot] \right\rangle - \left\langle \pi_t(\cdot|s), \mathbb{E}_{d_{P_t}^{\pi_t}} [r_t(\tau)|s, \cdot] \right\rangle \right) \\ 1232 &= \sum_{t=1}^T \left\langle \pi_{t+1}(\cdot|s) - \pi_t(\cdot|s), \mathbb{E}_{d_{P_t}^{\pi_t}} [r_t(\tau)|s, \cdot] \right\rangle + \sum_{t=1}^T \left\langle \pi(\cdot|s) - \pi_{t+1}(\cdot|s, \cdot), \mathbb{E}_{d_{P_t}^{\pi_t}} [r_t(\tau)|s, \cdot] \right\rangle \\ 1233 &\leq \sum_{t=1}^T \left\langle \pi_{t+1}(\cdot|s) - \pi_t(\cdot|s, \cdot), \mathbb{E}_{d_{P_t}^{\pi_t}} [\hat{r}_t(\tau)|s, \cdot] \right\rangle - \psi_s(\pi_1), \end{aligned}$$

1239 where the last inequality is by Lemma C.1. This completes the proof.  $\square$

1242 **Lemma C.3.** Let  $\pi \in \Pi$  be an arbitrary policy. Then for any state  $s \in \mathcal{S}$ , if we set the learning rate  
 1243  $\eta = \sqrt{\frac{\log |\mathcal{A}|}{2R_{\max}^2 T}}$

1244  
 1245 
$$\sum_{t=1}^T \langle \pi(\cdot|s) - \pi_t(\cdot|s), \mathbb{E}_{d_{P_t}^{\pi_t}} [r_t(\tau)|s, \cdot] \rangle \leq 2R_{\max} \sqrt{2 \log |\mathcal{A}| T}.$$
  
 1246  
 1247

1248  
 1249 **Proof of Lemma C.3.** We define the surrogate objective accumulated over  $t$  iterations as  
 1250

1251 
$$\mathcal{F}_{s,t}(\pi) := \sum_{t=1}^T \langle \pi(\cdot|s), \mathbb{E}_{P_t} [r_t(\tau)|s, \cdot] \rangle - \psi_s(\pi).$$
  
 1252  
 1253

1254 Let  $B_{\mathcal{F}_{s,t}}(\cdot|\cdot)$  denote the Bergman divergence with respect to  $\mathcal{F}_{s,t}$ . By the definition of Bergman  
 1255 divergence, we have

1256 
$$\begin{aligned} \mathcal{F}_{s,t}(\pi_t) &= \mathcal{F}_{s,t}(\pi_{t+1}) + \langle \pi_t(\cdot|s) - \pi_{t+1}(\cdot|s), \nabla \mathcal{F}_{s,t}(\pi)|_{\pi=\pi_{t+1}} \rangle + B_{\mathcal{F}_{s,t}}(\pi_t\|\pi_{t+1}) \\ &\leq \mathcal{F}_{s,t}(\pi_{t+1}) + B_{\mathcal{F}_{s,t}}(\pi_t\|\pi_{t+1}) \\ &= \mathcal{F}_{s,t}(\pi_{t+1}) - B_{\psi_s}(\pi_t\|\pi_{t+1}) \\ &\Rightarrow B_{\psi_s}(\pi_t\|\pi_{t+1}) \leq \mathcal{F}_{s,t}(\pi_{t+1}) - \mathcal{F}_{s,t}(\pi_t) \\ &\leq \left\langle \pi_{t+1}(\cdot|s) - \pi_t(\cdot|s), \mathbb{E}_{d_{P_t}^{\pi_t}} [r_t(\tau)|s, \cdot] \right\rangle, \end{aligned}$$
  
 1257  
 1258  
 1259  
 1260  
 1261  
 1262  
 1263

1264 where the second step is because  $\pi_t$  is the maximizer of  $\mathcal{F}_{s,t}$ , and the gradient term is non-positive,  
 1265 the third step is because both  $\mathcal{F}_{s,t}$  and  $\psi_s(\pi)$  are linear and convex, we have:  $B_{\mathcal{F}_{s,t}}(\pi_t\|\pi_{t+1}) =$   
 1266  $-B_{\psi_s}(\pi_t\|\pi_{t+1})$ .

1267 To convert the Bergman divergence into a squared norm, we follow [Xie et al., 2021] by applying the  
 1268 second-order Taylor expansion

1269  
 1270 
$$B_{\psi_s}(\pi_t\|\pi_{t+1}) = \frac{1}{2} \|\pi_t(\cdot|s) - \pi_{t+1}(\cdot|s)\|_{H_{\psi_s}(\pi'_t)}^2,$$
  
 1271

1272 where  $\pi'_t := \alpha\pi_t + (1 - \alpha)\pi_{t+1}$  for some  $\alpha \in [0, 1]$ , and  $H_{\psi_s}$  is the hessian of  $\psi_s$ .  
 1273

1274 Using Cauchy–Schwarz inequality

1275  
 1276 
$$\left\langle \pi_{t+1} - \pi_t, \mathbb{E}_{d_{P_t}^{\pi_t}} [r_t(\tau)|s] \right\rangle \leq \|\pi_{t+1} - \pi_t\|_{H_{\psi_s}(\pi'_t)} \cdot \left\| \mathbb{E}_{d_{P_t}^{\pi_t}} [r_t(\tau)|s, \cdot] \right\|_{H_{\psi_s}^{-1}(\pi'_t)}.$$
  
 1277

1278 From the Hessian of  $\psi_s$ , it is known that

1279  
 1280 
$$\left\| \mathbb{E}_{d_{P_t}^{\pi_t}} [r_t(\tau)|s] \right\|_{H_{\psi_s}^{-1}} \leq \sqrt{\eta} \left\| \mathbb{E}_{d_{P_t}^{\pi_t}} [r_t(\tau)|s] \right\|_{\infty} \leq \sqrt{\eta} R_{\max}.$$
  
 1281

1282 Combining everything

1283  
 1284 
$$\begin{aligned} \left\langle \pi_{t+1} - \pi_t, \mathbb{E}_{d_{P_t}^{\pi_t}} [r_t(\tau)|s, \cdot] \right\rangle &\leq \sqrt{2B_{\psi_s}(\pi_t\|\pi_{t+1})} \cdot \sqrt{\eta} R_{\max} \\ 1285 \Rightarrow \left\langle \pi_{t+1} - \pi_t, \mathbb{E}_{d_{P_t}^{\pi_t}} [r_t(\tau)|s, \cdot] \right\rangle &\leq \sqrt{2} \left\langle \pi_{t+1} - \pi_t, \mathbb{E}_{d_{P_t}^{\pi_t}} [r_t(\tau)|s, \cdot] \right\rangle \cdot \sqrt{\eta} R_{\max} \\ 1286 \Rightarrow \left\langle \pi_{t+1} - \pi_t, \mathbb{E}_{d_{P_t}^{\pi_t}} [r_t(\tau)|s, \cdot] \right\rangle &\leq 2\eta R_{\max}^2 \\ 1287 \sum_{t=1}^T \left\langle \pi_{t+1} - \pi_t, \mathbb{E}_{d_{P_t}^{\pi_t}} [r_t(\tau)|s, \cdot] \right\rangle &\leq 2\eta R_{\max}^2 T. \end{aligned}$$
  
 1288  
 1289  
 1290  
 1291

1292 By Lemma C.2, we have  
 1293

1294  
 1295 
$$\sum_{t=1}^T \langle \pi - \pi_t, \mathbb{E}_{d_{P_t}^{\pi_t}} [r_t(\tau)|s, \cdot] \rangle \leq \sum_{t=1}^T \langle \pi_{t+1} - \pi_t, \mathbb{E}_{d_{P_t}^{\pi_t}} [r_t(\tau)|s, \cdot] \rangle - \psi_s(\pi_1)$$

$$\leq 2\eta R_{\max}^2 T + \frac{\log |\mathcal{A}|}{\eta},$$

where the second step is because  $\pi_1$  is the uniform policy. Choosing  $\eta = \sqrt{\frac{\log |\mathcal{A}|}{2R_{\max}^2 T}}$  concludes the proof.  $\square$

**Lemma C.4.** Let  $\pi^{\text{ALG}} = \text{argmax}_{\pi: \mathcal{S} \rightarrow \Delta(\mathcal{A})} \sum_{t=1}^T J_{\mathcal{M}_t}(\pi) - J_{\mathcal{M}_t}(\pi_t)$  and  $\eta = \sqrt{\frac{\log |\mathcal{A}|}{2R_{\max}^2 T}}$ , we have

$$\mathfrak{R}_T \leq 2R_{\max} \sqrt{2T \log |\mathcal{A}|}.$$

**Proof of Lemma C.4.** Please recall that  $J_{\mathcal{M}_t}(\pi) = J(\pi, r_t, P_t)$ . We apply the standard performance difference Lemma Kakade & Langford [2002], which gives

$$\begin{aligned} \mathfrak{R}_T &= \sum_{t=1}^T J_{\mathcal{M}_t}(\pi^{\text{ALG}}) - J_{\mathcal{M}_t}(\pi_t) = \sum_{t=1}^T \mathbb{E}_{d_{P_t}^{\pi^{\text{ALG}}}} \left[ \mathbb{E}_{d_{P_t}^{\pi^{\text{ALG}}}} [r_t(\tau) | s, \cdot] - \mathbb{E}_{d_{P_t}^{\pi^{\text{ALG}}}} [r_t(\tau) | s, \cdot] \right] \\ &= \sum_{t=1}^T \mathbb{E}_{d_{P_t}^{\pi^{\text{ALG}}}} \left[ \langle \pi^{\text{ALG}}(\cdot | s) - \pi_t(\cdot | s), \mathbb{E}_{d_{P_t}^{\pi^{\text{ALG}}}} [r_t(\tau) | s, \cdot] \rangle \right] \\ &\leq 2R_{\max} \sqrt{2T \log |\mathcal{A}|}, \end{aligned}$$

where the last step is by Lemma C.3. This completes the proof.  $\square$

## D TECHNICAL PROOFS FOR KNRs

In the Kernelized Nonlinear Regulator (KNR) setting, the structural constraint is imposed on the transition probability model, rather than the reward model. Consequently, we focus on modifying the related Lemmas on the transition model accordingly. Before we begin, let's recall some definitions and notations for better readability.

### Summarization of Notations:

- We use  $d$  to represents the dimension of the feature mapping  $\phi(s, a)$ , while  $d'$  denotes the dimension of the state space  $\mathcal{S}$ .
- $\Sigma_n = \sum_{i=1}^n \phi(s_i, a_i) \phi(s_i, a_i)^\top + \lambda I$ ,  $\Sigma_\pi = \mathbb{E}_{(s, a) \sim d^\pi} [\phi(s, a) \phi(s, a)^\top]$ , and  $\Sigma_\mu = \mathbb{E}_{(s, a) \sim \mu} [\phi(s, a) \phi(s, a)^\top]$ .
- Relative condition number:  $\mathfrak{C}_P^K(\pi) = \sup_{x \in \mathbb{R}^d} \left( \frac{x^\top \Sigma_\pi x}{x^\top \Sigma_\mu x} \right)$ .

**Lemma D.1.** Let  $\phi: \mathcal{S} \times \mathcal{A} \rightarrow \mathbb{R}^d$  be a feature mapping with  $\|\phi(s, a)\|_2 \leq 1$ , and define the KNR transition model class

$$\mathcal{F}_{\text{KNR}} := \{f_W(s, a) = W\phi(s, a) : \|W\|_F \leq L\}, \quad W \in \mathbb{R}^{d' \times d},$$

where  $d'$  is the dimension of the state space.

The following cover number bounds hold

$$\begin{aligned} \log \mathcal{N}_\infty(\{\mathcal{P}_h\}_{h=0}^{H-1}, 1/N) &\leq \text{rank}(\Sigma_\mu) d' \log(1 + 2LN) := \mathbb{N}_\mathcal{P}. \\ \log \mathcal{N}_\infty(\mathcal{R}, 1/N) &\leq \text{rank}(\Sigma_\mu) \log(1 + 2N) := \mathbb{N}_\mathcal{R}. \end{aligned}$$

**Proof of Lemma D.1.** We begin with the observation that for any  $W \in \mathbb{R}^{d' \times d}$ , the function  $f_W(s, a) := W\phi(s, a)$  is linear in  $\phi(s, a)$ .

Let  $\mathcal{H}_\mu := \text{Im}(\Sigma_\mu) \subseteq \mathbb{R}^d$  be the image of  $\Sigma_\mu$ , and let  $r = \dim(\mathcal{H}_\mu) = \text{rank}(\Sigma_\mu)$ . By the definition of image, we have

$$\mathcal{H}_\mu = \text{Span} \{ \phi(s, a) : (s, a) \in \Delta(\mu) \}.$$

1350 Hence, every  $\phi(s, a)$  lies in  $\mathcal{H}_\mu$ , and there exists an orthonormal matrix  $U \in \mathbb{R}^{d \times r}$  whose columns  
 1351 form a basis for  $\mathcal{H}_\mu$ , such that

$$1352 \quad \phi(s, a) = Uz(s, a), \quad z(s, a) \in \mathbb{R}^r.$$

1353 Substituting into the function expression, we obtain

$$1355 \quad f_W(s, a) = W\phi(s, a) = WUz(s, a).$$

1356 Define  $\tilde{W} := WU \in \mathbb{R}^{d' \times r}$ . Then we can rewrite

$$1358 \quad f_W(s, a) = \tilde{W}z(s, a).$$

1359 Because  $U$  has orthonormal columns, we have

$$1361 \quad \|\tilde{W}\|_F = \|WU\|_F \leq \|W\|_F \cdot \|U\|_2 = \|W\|_F,$$

1362 where  $\|U\|_2 = 1$ . Therefore, if  $\|W\|_F \leq L$ , then  $\|\tilde{W}\|_F \leq L$ .

1363 Thus, the function class  $\mathcal{F}_{\text{KNR}}$  is equivalent to the reduced class

$$1365 \quad \tilde{\mathcal{F}} := \left\{ (s, a) \mapsto \tilde{W}z(s, a) : \tilde{W} \in \mathbb{R}^{d' \times r}, \|\tilde{W}\|_F \leq L \right\}.$$

1366 By Example 5.8 in Section 5 of [Wainwright \[2019\]](#), we have that

$$1369 \quad \log \mathcal{N}(\tilde{\mathcal{F}}, \epsilon) \leq rd' \log \left( 1 + \frac{2L}{\epsilon} \right).$$

1370 This completes the proof. □

1373 **Lemma D.2.** *With probability at least  $1 - \delta$ , we have*

$$1375 \quad \mathcal{E}_2(\{P_h^*\}_{h=0}^{H-1}; \mathcal{D}) = \frac{1}{N} \sum_{n=1}^N \sum_{h=0}^{H-1} \sum_{i=0}^1 \left\| P_h^*(s_{h+1}^{n,i} | s_h^{n,i}, a_h^{n,i}) - \hat{P}_h(s_{h+1}^{n,i} | s_h^{n,i}, a_h^{n,i}) \right\| \\ 1376 \quad \leq \frac{c_1 \xi}{\zeta} \left( H \lambda_{\Sigma_n^{-1}} \sqrt{\frac{\log(2HN\mathcal{P}/\delta)}{N}} + H\Gamma(N, \delta) \right),$$

1381 where  $\xi = c_1 \sqrt{\|W^*\|_2 + d' \text{rank}(\Sigma_\mu) \{ \text{rank}(\Sigma_\mu) + \log(c_2/\delta) \} \log(1 + N)}$ ,  $\Gamma(N, \delta) =$   
 1382  $\sqrt{\frac{\text{rank}(\Sigma_\mu) \{ \text{rank}(\Sigma_\mu) + \ln(c_2/\delta) \}}{N}}$ ,  $c_1$  and  $c_2$  are universal constants.

1383

1384

1385 **Proof of Lemma D.2.** By the definition of the regularization term, we have

$$1387 \quad \mathcal{E}_2(\{P_h^*\}_{h=0}^{H-1}; \mathcal{D}) = \frac{1}{N} \sum_{n=1}^N \sum_{h=0}^{H-1} \sum_{i=0}^1 \left\| P_h^*(s_{h+1}^{n,i} | s_h^{n,i}, a_h^{n,i}) - \hat{P}_h(s_{h+1}^{n,i} | s_h^{n,i}, a_h^{n,i}) \right\|.$$

1389 Substitute the KNR matrix into the equation above

$$1392 \quad \mathcal{E}_2(\{P_h^*\}_{h=0}^{H-1}; \mathcal{D}) \leq \frac{1}{N\zeta} \sum_{n=1}^N \sum_{h=0}^{H-1} \sum_{i=0}^1 \|(W^* - \hat{W})\phi(s_h^{n,i}, a_h^{n,i})\|_2 \\ 1393 \quad \leq \frac{1}{N\zeta} \sum_{n=1}^N \sum_{h=0}^{H-1} \sum_{i=0}^1 \left\| (W^* - \hat{W})\Sigma_n^{1/2} \right\|_2 \cdot \left\| \phi(s_h^{n,i}, a_h^{n,i}) \right\|_{\Sigma_n^{-1}} \\ 1394 \quad \leq \frac{\xi}{N\zeta} \sum_{n=1}^N \sum_{h=0}^{H-1} \sum_{i=0}^1 \left\| \phi(s_h^{n,i}, a_h^{n,i}) \right\|_{\Sigma_n^{-1}},$$

1400 where the first step is by Lemma 13 in [Uehara & Sun \[2021b\]](#), the second step is by Cauchy-Schwarz  
 1401 inequality, and the last step is by Lemma 12 in [Uehara & Sun \[2021b\]](#), i.e.,

$$1403 \quad \left\| (W^* - \hat{W})\Sigma_n^{1/2} \right\|_2 \leq c_1 \sqrt{\|W^*\|_2 + d' \text{rank}(\Sigma_\mu) \{ \text{rank}(\Sigma_\mu) + \log(c_2/\delta) \} \log(1 + N)} = \xi.$$

1404 We assume that:  $Z_\phi := \sum_{h=0}^{H-1} \sum_{i=0}^1 \left\| \phi(s_h^{n,i}, a_h^{n,i}) \right\|_{\Sigma_n^{-1}}$ , so we have  
 1405

$$1406 \quad 1407 \quad 1408 \quad 1409 \quad \mathcal{E}_2(\{P_h^*\}_{h=0}^{H-1}; \mathcal{D}) \leq \frac{\xi}{\zeta} \frac{1}{N} \sum_{n=1}^N Z_\phi.$$

1410 We also assume: Each  $\phi(s, a) \in \mathbb{R}^d$  satisfies  $\|\phi(s, a)\|_2 \leq 1$ , so we have  
 1411

$$1412 \quad \|\phi(s, a)\|_{\Sigma_n^{-1}} \leq \sqrt{\lambda_{\max}(\Sigma_n^{-1})} \cdot \|\phi(s, a)\|_2 = \sqrt{\lambda_{\max}(\Sigma_n^{-1})} := \lambda_{\Sigma_n^{-1}}.$$

1413 From theorem 21 in [Chang et al. \[2021\]](#), with probability at least  $1 - \delta$ , we have  
 1414

$$1415 \quad 1416 \quad 1417 \quad \mathbb{E}_{(s,a) \sim \mu} [\|\phi(s, a)\|_{\Sigma_n^{-1}}] \leq c_1 \sqrt{\frac{\text{rank}[\Sigma_\mu] \{\text{rank}[\Sigma_\mu] + \ln(c_2/\delta)\}}{N}} = c_1 \Gamma(N, \delta).$$

1418 By applying Hoeffding's inequality and union bound, we have  
 1419

$$1420 \quad 1421 \quad 1422 \quad \mathbb{P} \left( \left| \frac{1}{N} \sum_{n=1}^N Z_\phi^{(n)} - \mathbb{E}[Z_\phi] \right| \geq \epsilon \right) \leq 2H\mathbb{N}_P \cdot \exp \left( -\frac{N\epsilon^2}{2H^2\lambda_{\Sigma_n^{-1}}^2} \right),$$

$$1423 \quad 1424 \quad 1425 \quad \epsilon = H\lambda_{\Sigma_n^{-1}} \sqrt{\frac{2 \log(2H\mathbb{N}_P/\delta)}{N}}.$$

1426 By Lemma [B.4](#), we have  
 1427

$$1428 \quad \mathcal{E}_2(\{P_h^t\}_{h=0}^{H-1}; \mathcal{D})$$

$$1429 \quad 1430 \quad 1431 \quad \leq \frac{cHR_{\max}M_P^K}{\lambda_2} \sqrt{\frac{\log(H\mathbb{N}_P/\delta)}{N}} + \frac{c\xi}{\zeta} \left( H\lambda_{\Sigma_n^{-1}} \sqrt{\frac{\log(H\mathbb{N}_P/\delta)}{N}} + H\Gamma(N, \delta) \right).$$

1432 This completes the proof. □  
 1433

1434  
 1435 Now we want to modify Lemma [B.1](#) to the KNR setting. Specifically, we only need to modify the  
 1436 first term because that is the constraint of the KNR method, i.e, now we want to bound the term  
 1437

$$1438 \quad 1439 \quad \sum_{h=0}^{H-1} \mathbb{E}_{(s,a) \sim d_h^\pi} [D_{TV}(P_h^t(\cdot|s, a), P_h^*(\cdot|s, a))].$$

1440 **Lemma D.3.** *Let  $\pi$  be an arbitrary policy that belongs to  $\Pi$ . Then for the transition model  $\{P_h^t\}_{h=0}^{H-1}$   
 1441 selected in Line 5 of [Algorithm 1](#) corresponding to  $\pi_t$ , with probability at least  $1 - \delta$ , the following  
 1442 holds*

$$1444 \quad 1445 \quad 1446 \quad \sum_{h=0}^{H-1} \mathbb{E}_{(s,a) \sim d_h^\pi} [D_{TV}(P_h^t(\cdot|s, a), P_h^*(\cdot|s, a))]$$

$$1447 \quad 1448 \quad 1449 \quad \leq cH\mathfrak{C}_P^K(\pi) \left( \frac{R_{\max}M_P^K}{\lambda_2} \sqrt{\frac{\log(H\mathbb{N}_P/\delta)}{N}} + \frac{\xi}{\zeta} \left( \lambda_{\Sigma_n^{-1}} \sqrt{\frac{\log(H\mathbb{N}_P/\delta)}{N}} + \Gamma(N, \delta) \right) \right),$$

1450 where  $c > 0$  is a universal constant.

1451 **Proof of Lemma D.3.** We can start by decomposing the term above  
 1452

$$1453 \quad 1454 \quad 1455 \quad \sum_{h=0}^{H-1} \mathbb{E}_{(s,a) \sim d_h^\pi} [D_{TV}(P_h^t(\cdot|s, a), P_h^*(\cdot|s, a))]$$

$$1456 \quad 1457 \quad \leq \mathfrak{C}_P^K(\pi) \sum_{h=0}^{H-1} \mathbb{E}_{(s,a) \sim \mu_h} [D_{TV}(P_h^t(\cdot|s, a), P_h^*(\cdot|s, a))]$$

$$\begin{aligned}
& \leq \mathfrak{C}_P^K(\pi) \sum_{h=0}^{H-1} \left( \mathbb{E}_{(s,a) \sim \mu_h} \left[ \left\| P_h^t(\cdot|s,a) - \widehat{P}_h(\cdot|s,a) \right\|_{TV} \right] \right. \\
& \quad \left. + \mathbb{E}_{(s,a) \sim \mu_h} \left[ \left\| P_h^*(\cdot|s,a) - \widehat{P}_h(\cdot|s,a) \right\|_{TV} \right] \right).
\end{aligned}$$

We already have the bound for the second term, so what we need to do now is to achieve a bound for the first term. By Hoeffding's inequality and combined with Lemma D.2, we have

$$\begin{aligned}
& \mathbb{E}_{(s,a) \sim \mu_h} \left[ \left\| P_h^t(\cdot|s,a) - \widehat{P}_h(\cdot|s,a) \right\|_{TV} \right] \\
& \leq \frac{cR_{\max}M_P^K}{\lambda_2} \sqrt{\frac{\log(H\mathbb{N}_P/\delta)}{N}} + \frac{c\xi}{\zeta} \left( \lambda_{\Sigma_n^{-1}} \sqrt{\frac{\log(H\mathbb{N}_P/\delta)}{N}} + \Gamma(N, \delta) \right),
\end{aligned}$$

where  $M_P^K = \max_{t \in [1:T]} \sup_{x \in \mathbb{R}^d} \left( \frac{x^\top \Sigma_{\pi_t} x}{x^\top \Sigma_\mu x} \right)$ . This completes the proof.  $\square$

Here is the proof of Theorem 5.1.

**Proof of Corollary 5.1.**

$$\begin{aligned}
& J(\pi) - J(\pi^{\text{ALG}}) \\
& = \frac{1}{T} \sum_{t=1}^T (J(\pi) - J(\pi_t)) \\
& \lesssim \frac{1}{T} \sum_{t=1}^T (J_{\mathcal{M}_t}(\pi) - J_{\mathcal{M}_t}(\pi_t)) + \lambda_1 \mathcal{E}_1(r^*; \mathcal{D}) + \lambda_2 \mathcal{E}_2(\{P_h^*\}_{h=0}^{H-1}; \mathcal{D}) \\
& \quad + \mathfrak{C}_R(\pi) \sqrt{\frac{\kappa^2 \log(\mathcal{N}_R(1/N)/\delta)}{N}} \\
& \quad + HR_{\max} \mathfrak{C}_P^K(\pi) \left( \frac{R_{\max}M_P^K}{\lambda_2} \sqrt{\frac{\log(H\mathbb{N}_P/\delta)}{N}} + \frac{\xi}{\zeta} \left( \lambda_{\Sigma_n^{-1}} \sqrt{\frac{\log(H\mathbb{N}_P/\delta)}{N}} + \Gamma(N, \delta) \right) \right) \\
& \lesssim R_{\max} \sqrt{\frac{\log |\mathcal{A}|}{T}} + \lambda_1 \mathcal{E}_1(r^*; \mathcal{D}) + \lambda_2 \mathcal{E}_2(\{P_h^*\}_{h=0}^{H-1}; \mathcal{D}) \\
& \quad + \mathfrak{C}_R(\pi) \sqrt{\frac{\kappa^2 \log(\mathcal{N}_R(1/N)/\delta)}{N}} \\
& \quad + HR_{\max} \mathfrak{C}_P^K(\pi) \left( \frac{R_{\max}M_P^K}{\lambda_2} \sqrt{\frac{\log(2H\mathbb{N}_P/\delta)}{N}} + \frac{\xi}{\zeta} \left( \lambda_{\Sigma_n^{-1}} \sqrt{\frac{\log(2H\mathbb{N}_P/\delta)}{N}} + \Gamma(N, \delta) \right) \right) \\
& \lesssim R_{\max} \sqrt{\frac{\log |\mathcal{A}|}{T}} + \lambda_1 \left( \sqrt{\frac{\kappa^2 \log(\mathbb{N}_R/\delta)}{N}} + R_{\max} \sqrt{\frac{\log(2\mathbb{N}_R/\delta)}{2N}} \right) \\
& \quad + \lambda_2 \frac{\xi}{\zeta} \left( H \lambda_{\Sigma_n^{-1}} \sqrt{\frac{\log(H\mathbb{N}_P/\delta)}{N}} + H \Gamma(N, \delta) \right) \\
& \quad + \mathfrak{C}_R(\pi) \sqrt{\frac{\kappa^2 \log(\mathcal{N}_R(1/N)/\delta)}{N}} \\
& \quad + HR_{\max} \mathfrak{C}_P^K(\pi) \left( \frac{R_{\max}M_P^K}{\lambda_2} \sqrt{\frac{\log(H\mathbb{N}_P/\delta)}{N}} + \frac{\xi}{\zeta} \left( \lambda_{\Sigma_n^{-1}} \sqrt{\frac{\log(H\mathbb{N}_P/\delta)}{N}} + \Gamma(N, \delta) \right) \right),
\end{aligned}$$

where the second step is by Lemma B.7, Lemma B.1, the third step is by Lemma C.4, Lemma B.8, Lemma D.3, and The last step is by Lemma D.2, Lemma B.5. Substituting  $\lambda_1 = \mathcal{O}(\mathfrak{C}_R(\pi))$ ,  $\lambda_2 = \mathcal{O}(R_{\max} \sqrt{\mathfrak{C}_P^K(\pi) M_P^K})$  completes the proof.  $\square$

1512 **E TECHNICAL PROOFS FOR FACTORED MODELS**  
 1513

1514 To begin with, we will introduce some notations that will be used in the proofs that follow.  
 1515

1516 **Summarization of Notations:**

1517 • Number of parameters for the transition functions  $L_p = \sum_{i=1}^d |\mathcal{A}| \cdot |\mathcal{B}|^{1+|\mathcal{P}_i|}$ .  
 1518

1519 • Modified Concentrability Coefficient  $\mathfrak{C}_P^F(\pi) = \max_{i \in [1:d]} \mathbb{E}_{(s,a) \sim \mu} \left[ \left( \frac{d\pi(s[\mathcal{P}_i], a)}{\mu(s[\mathcal{P}_i], a)} \right)^2 \right]$ .  
 1520

1521  
 1522 **Lemma E.1.** *Let  $P_h^*$  be the ground-truth transition dynamics at time steps  $h \in [0 : H - 1]$ , with  
 1523 probability at least  $1 - \delta$ , we have*  
 1524

1525 
$$\mathcal{E}_2(\{P_h^*\}_{h=0}^{H-1}; \mathcal{D}) = \frac{1}{N} \sum_{n=1}^N \sum_{h=0}^{H-1} \sum_{i=0}^1 \left\| P_h^*(s_{h+1}^{n,i} | s_h^{n,i}, a_h^{n,i}) - \hat{P}_h(s_{h+1}^{n,i} | s_h^{n,i}, a_h^{n,i}) \right\|$$
  
 1526 
$$\leq cH \sqrt{\frac{\log(HdL/\delta)}{N}} + cH \sqrt{\frac{dL \log(LNd/\delta)}{N}},$$
  
 1527

1528 where  $c > 0$  is a universal constant.  
 1529

1530 **Proof of Lemma E.1.** To start with, the following inequality holds  
 1531

1532 
$$\begin{aligned} & \sum_{h=0}^{H-1} \mathbb{E}_{(s,a) \sim \mu_h} [D_{TV}(\hat{P}_h(\cdot | s, a), P_h^*(\cdot | s, a))] \\ &= \sum_{h=0}^{H-1} \mathbb{E}_{(s,a) \sim \mu_h} \left[ \sum_i D_{TV}(\hat{P}_{i,h}(\cdot | s[\mathcal{P}_i], a), P_{i,h}^*(\cdot | s[\mathcal{P}_i], a)) \right] \\ &\leq \sum_{h=0}^{H-1} \sum_i \sqrt{\mathbb{E}_{(s,a) \sim \mu} [D_{TV}(\hat{P}_{i,h}(\cdot | s[\mathcal{P}_i], a), P_{i,h}^*(\cdot | s[\mathcal{P}_i], a))^2]} \\ &\leq cH \sqrt{\frac{dL \log(LNd/\delta)}{N}}, \end{aligned}$$
  
 1533

1534 where the second and third steps are by the definition of Factored models, and the last inequality is  
 1535 adapted from section C.5 in [Uehara & Sun \[2021b\]](#).  
 1536

1537 Define:  $Y_n := \sum_{h=0}^{H-1} \sum_{i=0}^1 \left\| P_h^*(\cdot | s_h^{n,i}, a_h^{n,i}) - \hat{P}_h(\cdot | s_h^{n,i}, a_h^{n,i}) \right\| \in [0, 4H]$ .  
 1538

1539 By Hoeffding's inequality and apply union bound, we have  
 1540

1541 
$$\Pr \left( \left| \frac{1}{N} \sum_{n=1}^N Y_n - \mathbb{E}[Y_n] \right| \geq \epsilon \right) \leq 2HdL \exp \left( \frac{-2N\epsilon^2}{(4H)^2} \right) \Rightarrow \epsilon = 4H \sqrt{\frac{\log(2HdL/\delta)}{2N}}.$$
  
 1542

1543 Then with probability at least  $1 - \delta$   
 1544

1545 
$$\mathcal{E}_2(\{P_h^*\}_{h=0}^{H-1}; \mathcal{D}) \leq cH \sqrt{\frac{\log(HdL/\delta)}{N}} + cH \sqrt{\frac{dL \log(LNd/\delta)}{N}}.$$
  
 1546

1547 Then by Lemma [B.4](#), we have  
 1548

1549 
$$\begin{aligned} & \mathcal{E}_2(\{P_h^t\}_{h=0}^{H-1}; \mathcal{D}) \\ &\lesssim \frac{HM_P^F R_{\max}}{\lambda_2} \sqrt{\frac{\log(HdL/\delta)}{N}} + H \sqrt{\frac{\log(HdL/\delta)}{N}} + H \sqrt{\frac{dL \log(LNd/\delta)}{N}}. \end{aligned}$$
  
 1550

1551 This completes the proof.  $\square$   
 1552

1566  
 1567 **Lemma E.2.** Let  $\pi$  be an arbitrary policy that belongs to  $\Pi$ . Then, for any transition dynamics  
 1568  $\{P_h^t\}_{h=0}^{H-1}$  selected in Line 5 of [Algorithm 1](#) corresponding to  $\pi_t$ , with probability at least  $1 - \delta$ , the  
 1569 following holds

1570 
$$\sum_{h=0}^{H-1} \mathbb{E}_{d_h^\pi} [D_{TV}(P_h^t(\cdot|s, a), P_h^*(\cdot|s, a))]$$
  
 1571 
$$\leq cH\mathfrak{C}_P^F(\pi) \left( \frac{R_{\max}M_P^F}{\lambda_2} \sqrt{\frac{\log(HdL/\delta)}{N}} + \sqrt{\frac{\log(HdL/\delta)}{N}} + \sqrt{\frac{dL\log(LNd/\delta)}{N}} \right),$$
  
 1572

1573 where  $c > 0$  is universal constant.  
 1574

1575 **Proof of Lemma E.2.** We start by decomposing the term above  
 1576

1577 
$$\sum_{h=0}^{H-1} \mathbb{E}_{d_h^\pi} [D_{TV}(P_h^t(\cdot|s, a), P_h^*(\cdot|s, a))]$$
  
 1578 
$$\leq \mathfrak{C}_P^F(\pi) \sum_{h=0}^{H-1} \left( \mathbb{E}_{(s,a) \sim \mu_h} \left[ \left\| P_h^t(\cdot|s, a) - \hat{P}_h(\cdot|s, a) \right\|_{TV} \right] \right.$$
  
 1579 
$$\left. + \mathbb{E}_{(s,a) \sim \mu_h} \left[ \left\| P_h^*(\cdot|s, a) - \hat{P}_h(\cdot|s, a) \right\|_{TV} \right] \right),$$
  
 1580

1581 where  $\mathfrak{C}_P^F(\pi) = \max_{i \in [1:d]} \mathbb{E}_{(s,a) \sim \mu} \left[ \left( \frac{d^\pi(s[\mathcal{P}_i], a)}{\mu(s[\mathcal{P}_i], a)} \right)^2 \right]$ .  
 1582

1583 By Hoeffding's inequality and combined with [Lemma E.1](#)  
 1584

1585 
$$\mathbb{E}_{(s,a) \sim \mu_h} \left[ \left\| P_h^t(\cdot|s, a) - \hat{P}_h(\cdot|s, a) \right\|_{TV} \right]$$
  
 1586 
$$\leq \frac{cM_P^F}{\lambda_2} \sqrt{\frac{\log(HdL/\delta)}{N}} + c\sqrt{\frac{\log(HdL/\delta)}{N}} + c\sqrt{\frac{dL\log(LNd/\delta)}{N}},$$
  
 1587

1588 where  $M_P^F = \max_{t \in [1:T]} \max_{i \in [1:d]} \mathbb{E}_{(s,a) \sim \mu} \left[ \left( \frac{d^{\pi_t}(s[\mathcal{P}_i], a)}{\mu(s[\mathcal{P}_i], a)} \right)^2 \right]$ . Combining all the terms above, we have  
 1589

1590 
$$\mathbb{E}_{(s,a) \sim d_h^\pi} \left[ \left\| P_h^t(\cdot|s, a) - P_h^*(\cdot|s, a) \right\|_{TV} \right]$$
  
 1591 
$$\leq \mathfrak{C}_P^F(\pi) \left( \frac{cR_{\max}M_P^F}{\lambda_2} \sqrt{\frac{\log(HdL/\delta)}{N}} + c\sqrt{\frac{\log(HdL/\delta)}{N}} + c\sqrt{\frac{dL\log(LNd/\delta)}{N}} \right).$$
  
 1592

1593 This completes the proof.  $\square$   
 1594

1595 Now we present the proof of the PAC bound for Factored Models.  
 1596

1597 **Proof of Theorem 5.2.**

1598 
$$J(\pi) - J(\pi^{\text{ALG}})$$
  
 1599 
$$= \frac{1}{T} \sum_{t=1}^T (J(\pi) - J(\pi_t))$$
  
 1600 
$$\lesssim \frac{1}{T} \sum_{t=1}^T (J_{\mathcal{M}_t}(\pi) - J_{\mathcal{M}_t}(\pi_t)) + \lambda_1 \mathcal{E}_1(r^*; \mathcal{D}) + \lambda_2 \mathcal{E}_2(\{P_h^*\}_{h=0}^{H-1}; \mathcal{D})$$
  
 1601 
$$+ HR_{\max} \mathfrak{C}_P^F(\pi) \left( \frac{R_{\max}M_P^F}{\lambda_2} \sqrt{\frac{\log(HdL/\delta)}{N}} + \sqrt{\frac{\log(HdL/\delta)}{N}} + \sqrt{\frac{dL\log(LNd/\delta)}{N}} \right)$$
  
 1602 
$$+ \mathfrak{C}_R(\pi) \sqrt{\frac{c\kappa^2 \log(rL_1/\delta)}{N}}$$
  
 1603

$$\begin{aligned}
& \lesssim R_{\max} \sqrt{\frac{\log |\mathcal{A}|}{T}} + \lambda_1 \mathcal{E}_1(r^*; \mathcal{D}) + \lambda_2 \mathcal{E}_2(\{P_h^*\}_{h=0}^{H-1}; \mathcal{D}) \\
& + HR_{\max} \mathfrak{C}_P^F(\pi) \left( \frac{R_{\max} M_P^F}{\lambda_2} \sqrt{\frac{\log(HdL/\delta)}{N}} + \sqrt{\frac{\log(HdL/\delta)}{N}} + \sqrt{d \frac{\log(LNd/\delta)}{N}} \right) \\
& + \mathfrak{C}_R(\pi) \sqrt{\frac{\kappa^2 \log(rL_1/\delta)}{N}} \\
& \lesssim R_{\max} \sqrt{\frac{\log |\mathcal{A}|}{T}} + \lambda_1 \left( \sqrt{\frac{\kappa^2 \log(rL/\delta)}{N}} + R_{\max} \sqrt{\frac{\log(rL/\delta)}{N}} \right) \\
& + \lambda_2 \left( H \sqrt{\frac{\log(dL/\delta)}{N}} + H \sqrt{\frac{dL \log(LNd/\delta)}{N}} \right) \\
& + HR_{\max} \mathfrak{C}_P^F(\pi) \left( \frac{R_{\max} M_P^F}{\lambda_2} \sqrt{\frac{\log(HdL/\delta)}{N}} + \sqrt{\frac{\log(HdL/\delta)}{N}} + \sqrt{dL \log(LNd/\delta)} \right) \\
& + \mathfrak{C}_R(\pi) \sqrt{\frac{\kappa^2 \log(rL_1/\delta)}{N}},
\end{aligned}$$

where the second step is by Lemma B.7, Lemma B.1, Lemma B.8, Lemma E.2, the third step is by Lemma C.4, and the last step is by Lemma B.5, Lemma E.1. Substituting  $\lambda_1 = \mathcal{O}(\mathfrak{C}_R(\pi))$ ,  $\lambda_2 = \mathcal{O}(R_{\max} \sqrt{\mathfrak{C}_P^F(\pi) M_P^F})$  completes the proof.  $\square$

1643  
1644  
1645  
1646  
1647  
1648  
1649  
1650  
1651  
1652  
1653  
1654  
1655  
1656  
1657  
1658  
1659  
1660  
1661  
1662  
1663  
1664  
1665  
1666  
1667  
1668  
1669  
1670  
1671  
1672  
1673

1674 **F EXPERIMENTAL SETUP**  
16751676 **F.1 CODE**  
16771678 Our implementation of Algorithm 2 is available at anonymous GitHub page:  
16791680 [https://anonymous.4open.science/r/Anonymous\\_ICLR/README.md](https://anonymous.4open.science/r/Anonymous_ICLR/README.md)  
16811682 **F.2 DATASETS**  
16831684 Our method is assessed using the Meta-World datasets introduced by Yu et al. [2020a], specifically  
1685 the medium-replay curated by Choi et al. [2024]. The primary set of experiments focuses on the  
1686 medium-replay dataset. A key advantage of these datasets is that policies cannot achieve good  
1687 performance when trained with incorrect reward signals (e.g., random or constant), making them  
1688 particularly well-suited for evaluating offline reinforcement learning approaches. This is important  
1689 because some offline RL agents may still exhibit seemingly successful behavior even under faulty  
1690 reward supervision. Further dataset-related information is available in Choi et al. [2024].  
16911692 Note that the abbreviation *BPT* indicates *button-press-topdown*.  
16931694 The medium-replay dataset used in our study, originally introduced by Choi et al. [2024], comprises  
1695 replay buffers created using SAC agents [Haarnoja et al., 2018], which exhibit an average success  
1696 performance around 50%. Detailed information on dataset sizes is provided in Table 4.  
16971698 Table 4: The sizes of Meta-World *medium-replay* datasets [Yu et al., 2020a].  
1699

Dataset	BPT	box-close	dial-turn	sweep	BPT-wall	sweep-into	drawer-open	lever-pull
Size ( $\times 10^5$ )	3.0	24.0	9.0	21.0	4.5	3.0	3.0	9.0

1700 **F.3 COMPUTATIONAL RESOURCES**  
17011702 Our experiments are conducted on a computational cluster equipped with an Intel(R) Xeon(R)  
1703 Platinum 8470Q CPU and an Nvidia GeForce RTX 5090 GPU. Each training session consists of  
1704 100,000 gradient steps, taking approximately 50 minutes to complete (with evaluation).  
1705

1728 **G IMPLEMENTATION DETAILS**  
17291730 **G.1 EXPERIMENTAL DETAIL OF BENCHMARKS**  
17311732 The Table 5 provides a comprehensive summary of the reward model configuration used across  
1733 benchmark implementations, along with the key experimental settings for algorithms including IQL  
1734 (represented as Oracle in the table), MR, PT, DPPO, IPL, and APPO. These settings cover essential  
1735 implementation details such as network architecture, optimizer type, learning rates, batch sizes, and  
1736 the number of training epochs, ensuring transparency and fairness in reproduction and comparison.  
17371738 Table 5: Implementation details of the reward model and the baselines.  
1739

1740 <b>Algorithm</b>	1741 <b>Component</b>	1742 <b>Value</b>
1743 <b>Reward model</b>	Optimizer	Adam Kingma & Ba [2014]
	Learning rate	1e-3
	Batch size	512
	$Q$	100
	Hidden layer dim	128
	Hidden layers	3
	Activation function	ReLU
	Final activation	Tanh
	Epochs	300
	# of ensembles	3
1744 <b>IQL Kostrikov et al. [2021]</b>	Reward from the ensemble models	Average
	Optimizer	Adam Kingma & Ba [2014]
	Critic, Actor, Value hidden dim	256
	Critic, Actor, Value hidden layers	2
	Critic, Actor, Value activation function	ReLU
	Critic, Actor, Value learning rate	0.5
	Mini-batch size	256
	Discount factor	0.99
	$\beta$	3.0
	$\tau$	0.7
1745 <b>MR Lee et al. [2021]</b>	Neural networks ( $Q, V, \pi$ )	3-layers, hidden dimension 256
	Activation	ReLU for hidden activations
	$Q, V, \pi$ optimizer	Adam with learning rate 3e-4
	Batch size	256
	Target network soft update	0.005
	$\beta$ (IQL advantage weight)	3.0
	$\tau$ (IQL expitile parameter)	0.7
1746 <b>PT Kim et al. [2023]</b>	Discount factor	0.99
	Optimizer	AdamW Loshchilov & Hutter [2017]
	# of layers	1
	# of attention heads	4
	Embedding dimension	256
1747 <b>DPPO An et al. [2023]</b>	Dropout rate	0.1
	Preference predictor	The same as PT Kim et al. [2023]
	Smoothness regularization $\nu$	1.0
	Smoothness sigma $m$	20
	Regularization $\lambda$	0.5
1748 <b>IPL Hejna &amp; Sadigh [2023]</b>	Optimizer	Adam Kingma & Ba [2014]
	Regularization $\lambda$	3e-4
	$Q, V, \pi$ arch	3x256d
	$\beta$	4.0
	$\tau$	0.7
	Subsample $s$	16
1749 <b>APPO Kang &amp; Oh [2025]</b>	Neural networks ( $Q, V, \pi$ )	3-layers, hidden dimension 256
	Activation	LeakyReLU for hidden activations
	$Q, V, \pi$ optimizer	Adam with learning rate 3e-4
	$\pi$ optimizer	Adam with learning rate 3e-5
	Batch size	256 transitions and 16 trajectory pairs
	Target network soft update	0.001
	Discount factor	0.99

1782 **G.2 BASIC EXPERIMENTAL DESIGN**  
1783

1784 The preference dataset is constructed by randomly drawing pairs of trajectory fragments, each  
1785 consisting of 25 time steps. Preference labels are assigned using the true reward: a label of (0,1) is  
1786 used if the total rewards of the two trajectories differ by more than 12.5; otherwise, both segments  
1787 receive an equal preference label of (0.5, 0.5). Performance is quantified by task-specific success  
1788 rates, which reflect whether the agent manages to complete the intended task. We report the average  
1789 performance and standard deviation of the policies of the last 5 training steps across 3 random seeds.  
1790

1791 **G.3 TRAINING DETAILS**  
1792

1793 In the following, we talk about the details of the model implementation. We firstly represent the  
1794 dynamics model as an ensemble of neural networks that output a Gaussian distribution over the next  
1795 state given the current state and action:

$$1796 \hat{P}(s' | s, a) = \mathcal{N}(\mu(s, a), \Sigma(s, a)).$$

1797  
1798 Following previous works [Rigter et al. \[2022\]](#); [Sun \[2023\]](#), during the initial maximum likelihood  
1799 model training (Line 3 of [Algorithm 2](#)) we train an ensemble of 7 such dynamics models and pick the  
1800 best 5 models based on the validation error on a held-out test set of 10000 transitions from the offline  
1801 dataset  $\mathcal{D}$ . Each model in the ensemble is a 4-layer feedforward neural network with 200 hidden units  
1802 per layer. We summarize the details of the algorithm in [Algorithm 2](#).  
1803

**Algorithm 2** Model-based Conservative Planning (MCP)

1804 **Input:** Offline dataset  $\mathcal{D}$ ; regularization parameters  $\lambda_1, \lambda_2, \lambda_b$ ; rollout length  $l$ ; sub-trajectory length  
1805  $h$ :

- 1806 1: Initialize the policy  $\pi_1$  as the uniform policy.
- 1807 2: **Learn reward:**  $\hat{r} = \arg \max_{r \in \mathcal{R}} \sum_{n=1}^N \log P_r(o = o^n | \tau^{n,1}, \tau^{n,0})$ .
- 1808 3: **Learn transition kernel:** for all  $h \in \{0, \dots, H-1\}$ ,
- 1809 
$$\hat{P}_h = \arg \max_{P_h \in \mathcal{P}_h} \sum_{n=1}^N \sum_{i=0}^1 \log P_h(s_{h+1}^{n,i} | s_h^{n,i}, a_h^{n,i}).$$
- 1810 4: **for**  $t = 1, 2, \dots, T$  **do**
- 1811 **(a) Model update:**
  - 1812 (i) Initialize the reward model  $r$  and transition kernel  $\{P_h\}_{h=0}^{H-1}$  with the MLE models  $\hat{r}$  and  
1813  $\{\hat{P}_h\}_{h=0}^{H-1}$ .
  - 1814 (ii) Collect a sub-trajectory  $\tau^{\text{sub}}$  from  $s_{\text{sub}}$  of length  $h$  and compute  $r(\tau^{\text{sub}})$ .
  - 1815 (iii) Roll out  $\pi_t$  from  $s_{\text{sub}}$  under  $\{P_h \in \mathcal{P}_h\}_{h=0}^{H-1}$  for  $l$  steps to obtain  $\tau^{\text{eval}}$ .
  - 1816 (iv) Solve for  $r_t$  and  $\{P_h^t\}_{h=0}^{H-1}$ :
- 1817 
$$\min_{r, \{P_h\}_{h=0}^{H-1}} \mathbb{E}_{d^{\pi_t} \{P_h\}_{h=0}^{H-1}} [r(\tau^{\text{eval}}) | s_{\text{sub}}] - r(\tau^{\text{sub}}) + \lambda_1 \mathcal{E}_1(r; \mathcal{D}) + \lambda_2 \mathcal{E}_2(\{P_h\}_{h=0}^{H-1}; \mathcal{D}).$$
- 1818 **(b) Policy update:**
  - 1819 (i) Initialize  $\pi \leftarrow \pi_t$ .
  - 1820 (ii) Sample a batch of  $(s, a)$  from  $\mathcal{D}$  and draw  $a' \sim \pi_t(\cdot | s)$ .
  - 1821 (iii) Obtain  $\pi_t^{\text{loc}}$  by
- 1822 
$$\arg \max_{\pi} \left\langle \pi(\cdot | s), \mathbb{E}_{d^{\pi_t} \{P_h^t\}_{h=0}^{H-1}} [r_t(\tau) | s, \cdot] \right\rangle - \lambda_b (a' - a)^2.$$
- 1823 (iv) Align  $\pi_t^{\text{loc}}(\cdot | s)$  with  $\pi_t(\cdot | s)$  by minimizing the KL divergence to obtain  $\pi_{t+1}$ .
- 1824 5: **end for**
- 1825 6: **Output:**  $\pi^{\text{ALG}} = \pi^T$ .

1833  
1834 In (a)(iii), we follow TD3-BC [\[Fujimoto & Gu, 2021\]](#) to include a regression-style behavior cloning  
1835 loss to push the policy towards favoring actions contained in the dataset. In (b)(iv), we leverage the  
subtle decremental training for KL-divergence trust region updating to avoid  $\pi_t^{\text{loc}}$  getting too close

1836 to  $\pi_t$ . To ensure a fair comparison with baseline methods, we follow the official implementation  
 1837 provided by [Choi et al. \[2024\]](#) for training our reward model. Specifically, the reward model is  
 1838 implemented as an ensemble of three fully connected neural networks, each consisting of three hidden  
 1839 layers with 128 units per layer. ReLU is used as the activation function for all hidden layers, and a  
 1840 Tanh activation is applied to the final output. The ensemble prediction is computed as the average of  
 1841 the individual network outputs.

1842  
1843 Table 6: Model architecture and hyperparameters.

	Component	Value
Our work	Neural networks $(r, P, \pi)$	3-layers, hidden dimension 256
	Activation	ReLU for hidden activations
	$\pi$ optimizer	Adam with learning rate 1e-4
	Batch size	256 transitions and 256 trajectory pairs
	$\lambda_1$	1*
	$\lambda_2$	0.01*
	$\lambda_b$	1*
	Rollout length $l$	3*
	Sub-trajectory length $h$	5*
	no. of model networks	7
	no. of elites	5
	model learning rate	3e-4

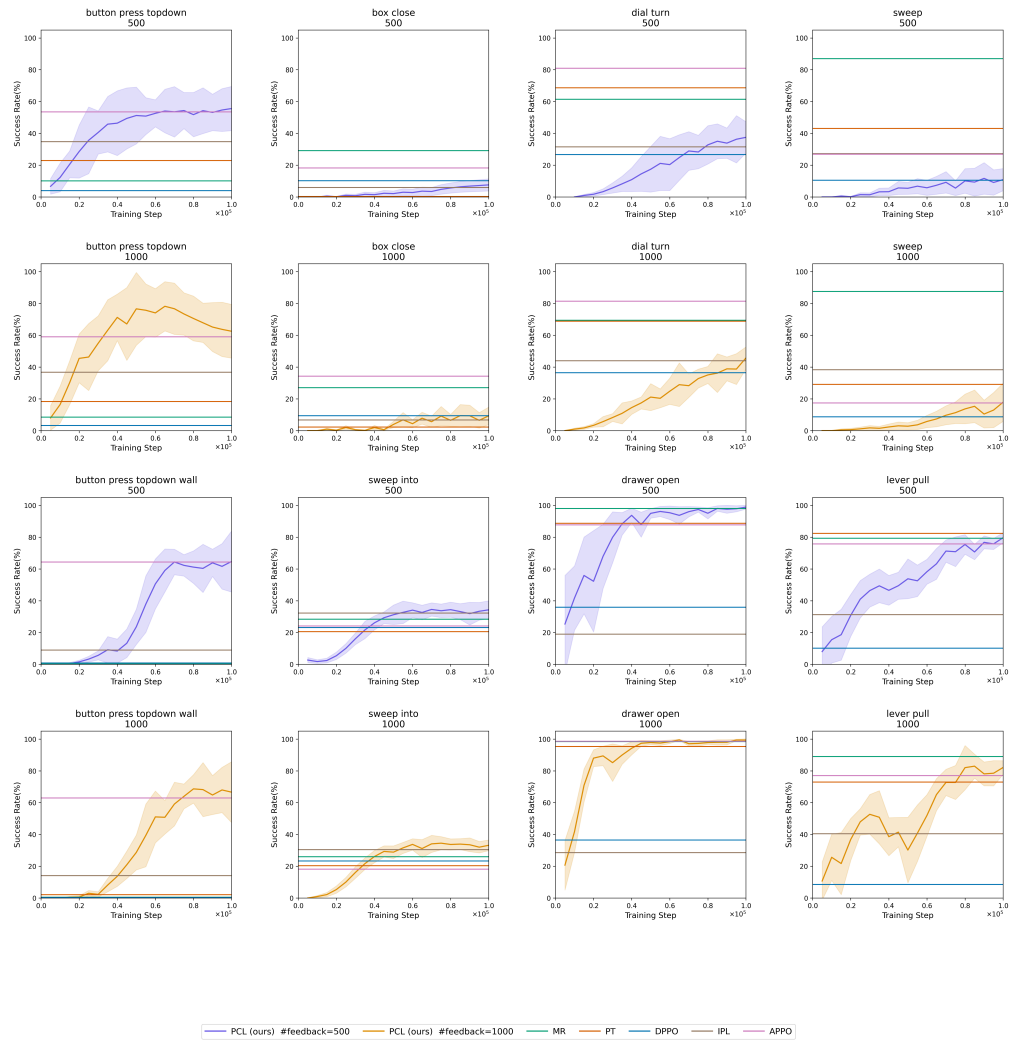
1858 \* The data marked with asterisks are only approximate values and need to be adjusted according to  
 1859 different datasets.  
 1860

1861 Table 7: Regularization hyperparameters used for MCP on each Meta-World task.  
1862

Task	$\lambda_1$	$\lambda_2$	$\lambda_b$
BPT	1e1	1e-5	3
box-close	1e-1	3e-3	3
sweep	1e1	1e-3	3
BPT-wall	1e1	1e-1	1
dial-turn	1e1	1e-2	3
sweep-into	3e-1	1e-1	3
drawer-open	1	3e-2	1
lever-pull	1	1e-2	1e-2

## 1890 H VISUALIZATION OF TRAINING DYNAMICS

1891  
 1892 Figure 3 illustrates the training progress corresponding to the experiments summarized in Table  
 1893 2. Each algorithm undergoes training for a total of 100,000 gradient update steps, during which  
 1894 performance evaluations are performed at regular intervals of every 5,000 steps. To derive the final  
 1895 success rate reported in the tables, we compute the average and standard deviation over the results  
 1896 from three random seeds, offering a more stable and representative performance estimate. This figure  
 1897 is generated from the mean, standard derivation of the success rates.  
 1898



1932 Figure 3: Learning curves from the experiments in Table 2 of main text.  
 1933

## 1936 I THE USE OF LLM

1937  
 1938 The authors used a large language model (LLM) to edit and polish the writing (grammar, wording,  
 1939 and clarity). All ideas, analyses, and conclusions are the authors' own.  
 1940

## 1941 J ADDITIONAL EXPERIMENTAL RESULTS

1944  
 1945  
 1946  
 1947  
 1948  
 1949  
 1950  
 1951  
 1952  
 1953

**Generalization to high-dimensional environments.** To evaluate the performance of MCP in more complex environments with significantly larger state–action spaces, we construct new offline PbRL datasets based on the MuJoCo tasks Ant [Schulman et al., 2015] and Humanoid [Tassa et al., 2012]. These two tasks have high-dimensional states and actions: Ant has a state space of dimension 105 (about 3 times larger than MetaWorld) and an action space of dimension 8 (about 2 times the action dimension of MetaWorld), while Humanoid has a state space of dimension 348 (about 9 times larger than MetaWorld) and an action space of dimension 17 (about 4 times the action dimension of MetaWorld). Table 8 reports the average total return over three seeds for each method. As shown in Table 8, MCP consistently outperforms MR and APPO on both high-dimensional tasks, demonstrating its potential in complex environments.

Table 8: Performance on high-dimensional MuJoCo tasks.

Algorithm	Oracle	MR	APPO	MCP
Humanoid	2672.48	1586.31	1365.34	1731.47
Ant	3007.22	1940.87	1638.42	2213.85

1960  
 1961  
 1962  
 1963  
 1964  
 1965

**Runtime analysis.** We measure the time required to perform 100k training steps using a single NVIDIA RTX 5090 GPU. As reported in Table 9, MCP is slightly slower than MR but still faster than APPO, while achieving better performance than both. Table 10 further decomposes the MCP runtime into the conservative planning step (line 5 of Algorithm 1) and the policy update step (line 6).

Table 9: Running time for 100k training steps.

Method	MR	APPO	MCP
Total time (min)	22.7	36.8	33.5

Table 10: Decomposition of MCP runtime for 100k training steps.

Method	MCP-step5	MCP-step6	MCP-total
Total time (min)	24.2	9.3	33.5

1972  
 1973  
 1974  
 1975  
 1976  
 1977  
 1978  
 1979  
 1980  
 1981

**Hyperparameter sensitivity.** We conduct a hyperparameter sensitivity analysis for the behavior cloning weights  $\lambda_b$  on the *drawer-open-1000* and *sweep-into-1000* tasks over three seeds.

Table 11: Sensitivity of MCP to regularization hyperparameters on *drawer-open-1000* and *sweep-into-1000*.

drawer-open-1000	$92.0 \pm 5.66$	$97.20 \pm 2.04$	$99.07 \pm 0.38$	$96.40 \pm 3.81$	$89.87 \pm 9.92$
sweep-into-1000	$22.53 \pm 7.39$	$26.8 \pm 4.25$	$29.2 \pm 6.76$	$34.13 \pm 3.27$	$31.6 \pm 5.02$